USGS
science for a changing world

Geochronologic and Geochemical Data from Metasedimentary and Associated Rocks in the Lane Mountain Area, San Bernardino County, California

Open-File Report 2022–1115

U.S. Department of the Interior
U.S. Geological Survey

Cover. Photograph of a metasedimentary rock outcrop in the Lane Mountain area, San Bernardino County, California. Rock is fine-grained calc-silicate hornfels assigned to the Noble Well formation of McCulloh (1960). Outcrop is 1 kilometer south of sample locality 14-LM-128, which yielded detrital zircons used for geochronological investigations in this report. U.S. Geological Survey photograph by Paul Stone.

Geochronologic and Geochemical Data from Metasedimentary and Associated Rocks in the Lane Mountain Area, San Bernardino County, California

By Paul Stone, M. Robinson Cecil, Howard J. Brown, and Jorge A. Vazquez

Open-File Report 2022–1115

U.S. Department of the Interior
U.S. Geological Survey

U.S. Geological Survey, Reston, Virginia: 2023

Suggested citation:
Stone, P., Cecil, M.R., Brown, H.J., and Vazquez, J.A., 2023, Geochronologic and geochemical data from metasedimentary and associated rocks in the Lane Mountain area, San Bernardino County, California: U.S. Geological Survey Open-File Report 2022–1115, 34 p., https://doi.org/10.3133/ofr20221115.

Associated data for this publication:
Stone, P., Cecil, M.R., and Vazquez, J.A., 2023, Tabular geochronologic and geochemical data from metasedimentary and associated rocks in the Lane Mountain area, San Bernardino County, California: U.S. Geological Survey data release, https://doi.org/10.5066/P9G6YNEF.

ISSN 2331-1258 (online)

Contents

Abstract....1
Introduction....1
Geographic Setting....4
Previous Investigations and Geologic Framework....4
Purpose and Scope....6
Methods....8
Detrital Zircon Geochronology....8
Carbide Formation....13
Unit Pcq_1....13
Sample 15-LM-921....13
Sample 15-LM-888....13
Sample 15-LM-883....13
Sample 18-LM-2738....13
Unit Pcmcg....14
Sample 16-LM-1215....14
Units Pch_1, Pcm, and Pcs_1....14
Sample 14-LM-60....14
Sample 15-LM-1012....14
Unit Pcq_2....14
Sample 15-LM-1085....14
Sample 15-LM-1173....14
Sample 15-LM-1050....14
Unit Pcu_1....15
Sample 15-LM-1135....15
Williams Well Formation....15
Sample 15-LM-894....15
Noble Well Formation....15
Samples 14-LM-128 and 15-LM-930....15
Samples 15-LM-909 and 15-LM-910....16
Unnamed Quartzite....16
Sample 16-LM-1342....16
Igneous and Metamorphic Zircon Geochronology....16
Quartzite with Metamorphic Zircons....19
Sample 17-LM-1349....19
Albitized Igneous Rocks....19
Samples 15-LM-600, 17-LM-2032, and 18-LM-2939....19
Fine-grained Intrusive Rocks....19
Samples 17-LM-1984 and 18-LM-2824....19
Geochemistry....20
Discussion....23
Detrital Zircon Overview....23
Detrital Zircon Stratigraphy....25
Carbide Formation....25
Williams Well and Starbright Formations....25

Noble Well Formation....25
Regional Detrital Zircon Comparisons....26
Implications for the El Paso Terrane....26
Summary....26
Acknowledgments....27
References Cited....27
Appendix 1—Excerpts from an Unpublished Manuscript by T.H. McCulloh....31
Appendix 2—Methods of U-Pb Zircon Geochronology....33

Figures

1. Map of north-central Mojave Desert region showing outcrops of El Paso terrane and location of report area....2
2. Map showing Sr_i = 0.706 isopleth in California and Nevada....3
3. Map showing general geology of Lane Mountain area and locations of samples included in report....5
4. Probability density curves and histograms of acceptable detrital zircon ages from samples 14-LM-60, 14-LM-128, 15-LM-883, 15-LM-888, and 15-LM-894....9
5. Probability density curves and histograms of acceptable detrital zircon ages from samples 15-LM-909, 15-LM-910, 15-LM-921, 15-LM-930, 15-LM-1012, 15-LM-1050, and 15-LM-1085....10
6. Probability density curves and histograms of acceptable detrital zircon ages from samples 15-LM-1085, 15-LM-1135, 15-LM-1173, 16-LM-1215, 16-LM-1342, and 18-LM-2738....11
7. Weighted mean age plots of youngest age clusters in detrital zircon samples 14-LM-60, 14-LM-128, 15-LM-883, 15-LM-888, 15-LM-894, 15-LM-909, 15-LM-910, 15-LM-921, 15-LM-930, 15-LM-1012, 15-LM-1050, 15-LM-1085, 15-LM-1135, 15-LM-1173, 16-LM-1215, and 17-LM-1342....12
8. Probability density curves and histograms of acceptable zircon ages from samples 15-LM-600, 17-LM-1349, 17-LM-1984, 17-LM-1984A, 17-LM-2032, 18-LM-2824, and 18-LM-2939....17
9. Weighted mean age plots of metamorphic zircons from quartzite sample 17-LM-1349, magmatic zircons from albitized igneous rock samples 15-LM-600, 17-LM-2302, and 18-LM-2939, combined, and magmatic zircons from fine-grained intrusive rock samples 17-LM-1984, 17-LM-1984A, and 18-LM-2824....18
10. Modified total alkali-silica diagram showing geochemical classification of albitized igneous rock samples of Permian age (15-LM-600, 17-LM-2032, and 18-LM-2939) and fine-grained intrusive rock samples of Jurassic age (17-LM-1984A and 18-LM-2824)....23
11. Composite probability density curves and histograms of zircon ages from all 17 detrital zircon samples analyzed for this report....24

Tables

1. Metasedimentary and metavolcanic rock units of McCulloh (1960) in Lane Mountain area....6
2. Location and other information for the 17 detrital zircon samples included in this report....7
3. Location and other information for the six non-detrital zircon samples included in this report....7
4. LA-SF-ICPMS U-Pb data for samples analyzed for this report, Lane Mountain area. (supplemental files accessible at https://doi.org/10.3133/ofr20221115)
5. SHRIMP-RG U-Pb zircon data for samples analyzed for this report, Lane Mountain area. (supplemental files accessible at https://doi.org/10.3133/ofr20221115)

6. Criteria for determining maximum depositional ages of detrital zircon samples included in this report..... 8
7. ICP-AES-MS and WDXRF geochemical analyses of samples included in this report..... 21

Conversion Factors

International System of Units to U.S. customary units

Multiply	By	To obtain
	Length	
centimeter (cm)	0.3937	inch (in.)
millimeter (mm)	0.03937	inch (in.)
meter (m)	3.281	foot (ft)
kilometer (km)	0.6214	mile (mi)
meter (m)	1.094	yard (yd)

Datum

Horizontal coordinate information is referenced to the North American Datum of 1927 (NAD27).

Abbreviations

ICP-AES-MS	inductively coupled plasma atomic emission spectroscopy-mass spectrometry
LA-SF-ICPMS	laser ablation sector field inductively coupled plasma mass spectrometry
Ma	mega-annum (a unit of time equivalent to one million years)
MSWD	mean squared weighted deviation
ppm	parts per million
SHRIMP-RG	sensitive high-resolution ion microprobe-reverse geometry
Sr_i	Initial $^{87}Sr/^{86}Sr$ ratio (Sr = Strontium)
WDXRF	wavelength dispersive x-ray fluorescence
YC1σ[2+]	weighted mean age of the youngest cluster of two or more zircon ages in a sample that overlap at one standard deviation
YPP	youngest zircon age peak (based on two or more ages) on a probability density curve
YSG	youngest single zircon grain age in a sample

Chemical Symbols

Ag	Silver
Al	Aluminum
As	Arsenic
B	Boron
Ba	Barium
Be	Beryllium
Bi	Bismuth
Ca	Calcium
Cd	Cadmium
Ce	Cerium
Co	Cobalt
Cr	Chromium
Cs	Cesium
Cu	Copper
Dy	Dysprosium
Er	Erbium
Eu	Europium
Fe	Iron
Ga	Gallium
Gd	Gadolinium
Ge	Germanium
Hf	Hafnium
Ho	Holmium
In	Indium
K	Potassium
La	Lanthanum
Li	Lithium
Lu	Lutetium
Mg	Magnesium
Mn	Manganese
Mo	Molybdenum
Nb	Niobium
Nd	Neodymium
Ni	Nickel
O	Oxygen
P	Phosphorus
Pb	Lead
Pr	Praseodymium
Rb	Rubidium
S	Sulfur
Sb	Antimony
Sc	Scandium
Se	Selenium
Si	Silicon
Sm	Samarium
Sn	Tin
Sr	Strontium
Ta	Tantalum
Tb	Terbium
Te	Tellurium
Th	Thorium
Ti	Titanium
Tl	Thallium
Tm	Thulium
U	Uranium
V	Vanadium
W	Tungsten
Y	Yttrium
Yb	Ytterbium
Zn	Zinc
Zr	Zirconium

Geochronologic and Geochemical Data from Metasedimentary and Associated Rocks in the Lane Mountain Area, San Bernardino County, California

By Paul Stone,[1] M. Robinson Cecil,[2] Howard J. Brown,[3] and Jorge A. Vazquez[1]

Abstract

Eugeoclinal metasedimentary and metavolcanic rocks in the Lane Mountain area, California, are considered part of the El Paso terrane, which is commonly thought to have been displaced several hundred kilometers (km) southeastward from its place of origin during late Paleozoic truncation of the North American continental margin. Uranium-lead dating of detrital zircons from this area was undertaken to limit the depositional ages of these nearly non-fossiliferous metamorphic rocks. Analysis of detrital zircons from 17 metasedimentary rock samples yielded a composite age distribution that ranges from Archean to Jurassic and has significant peaks at ~2,800–2,400 mega-annum (Ma), 2,100–1,600 Ma, and ~300–200 Ma. The Proterozoic and Archean ages indicate derivation from continental sources in ancestral North America, whereas the late Paleozoic and Mesozoic ages are interpreted as derived from a magmatic arc that began to develop along the continental margin in Permian to Triassic time.

The 17 detrital zircon samples are from quartzitic and conglomeratic rocks of the Carbide, Williams Well, and Noble Well formations, which were informally named by T.H. McCulloh in 1960. The zircon data indicate that the oldest rocks in the Carbide formation are quartzites likely correlative with the Ordovician Eureka Quartzite of the Cordilleran miogeocline. These rocks lie structurally above the rest of the Carbide formation, different units of which yielded zircons that indicate maximum depositional ages ranging from middle Paleozoic to Late Triassic. Zircons from the Williams Well and Noble Well formations indicate maximum depositional ages of late Paleozoic and Early Jurassic, respectively. The Noble Well formation is interpreted to correlate with the lithologically similar, Early Jurassic, Fairview Valley Formation of the Black and Quartzite Mountain areas some 60 km to the southwest.

The above interpretations depend on the presumption that the detrital zircons in these samples did not undergo extreme, post-depositional lead loss, which would result in misleadingly young ages. Although such lead loss is considered unlikely for these samples, further work could test the validity of this interpretation.

Zircons from six additional samples were also analyzed: (1) a quartzite from which all the zircons are interpreted to have formed by Late Jurassic metamorphism; (2) three samples interpreted as albitized igneous rocks of Middle Permian age; and (3) two samples interpreted as fine-grained monzonite to diorite of Late Jurassic age. Both sets of igneous rocks were initially thought to be metasedimentary but were reinterpreted as igneous largely on the basis of the zircon data.

Based on the interpretations presented here, this study demonstrates that the depositional, magmatic, and deformational history of the El Paso terrane was longer and more complex than previously thought and will require reevaluation of existing tectonic models involving this terrane.

Introduction

The Lane Mountain area is about 20 kilometers (km) northeast of Barstow, California, in the north-central Mojave Desert (fig. 1), a region of complex and incompletely understood geology. In this region, metasedimentary and metavolcanic rocks of offshore (eugeoclinal) lithologic character (McCulloh, 1952, 1960; Miller and Sutter, 1982; Carr and others, 1997) are intruded by a variety of plutonic rocks, some of which are characterized by initial $^{87}Sr/^{86}Sr$ (Sr_i)[4] values <0.706 and other isotopic signatures that indicate little Precambrian continental (sialic) lithosphere in their magmatic source areas (Kistler, 1990; Miller and others, 1995). The eugeoclinal metasedimentary and metavolcanic rocks of this region, including those of the Lane Mountain area, compose the El Paso terrane of Silberling and others (1987, 1992; fig. 1), which many have interpreted as significantly displaced from its original location (for example, Burchfiel and Davis, 1981; Miller and others, 1995; Saleeby and Dunne, 2015). The associated low-Sr_i plutonic rocks form a narrow, northwest-trending belt that is surrounded by plutonic rocks with Sr_i >0.706 and is bisected and offset by the late Cenozoic, left-lateral Garlock Fault (Kistler and Ross, 1990; fig. 2). Although this general

[1]U.S. Geological Survey.

[2]California State University Northridge.

[3]Apple Valley, California.

[4] Chemical element symbols used in this paper are listed in the preface (p. vi)

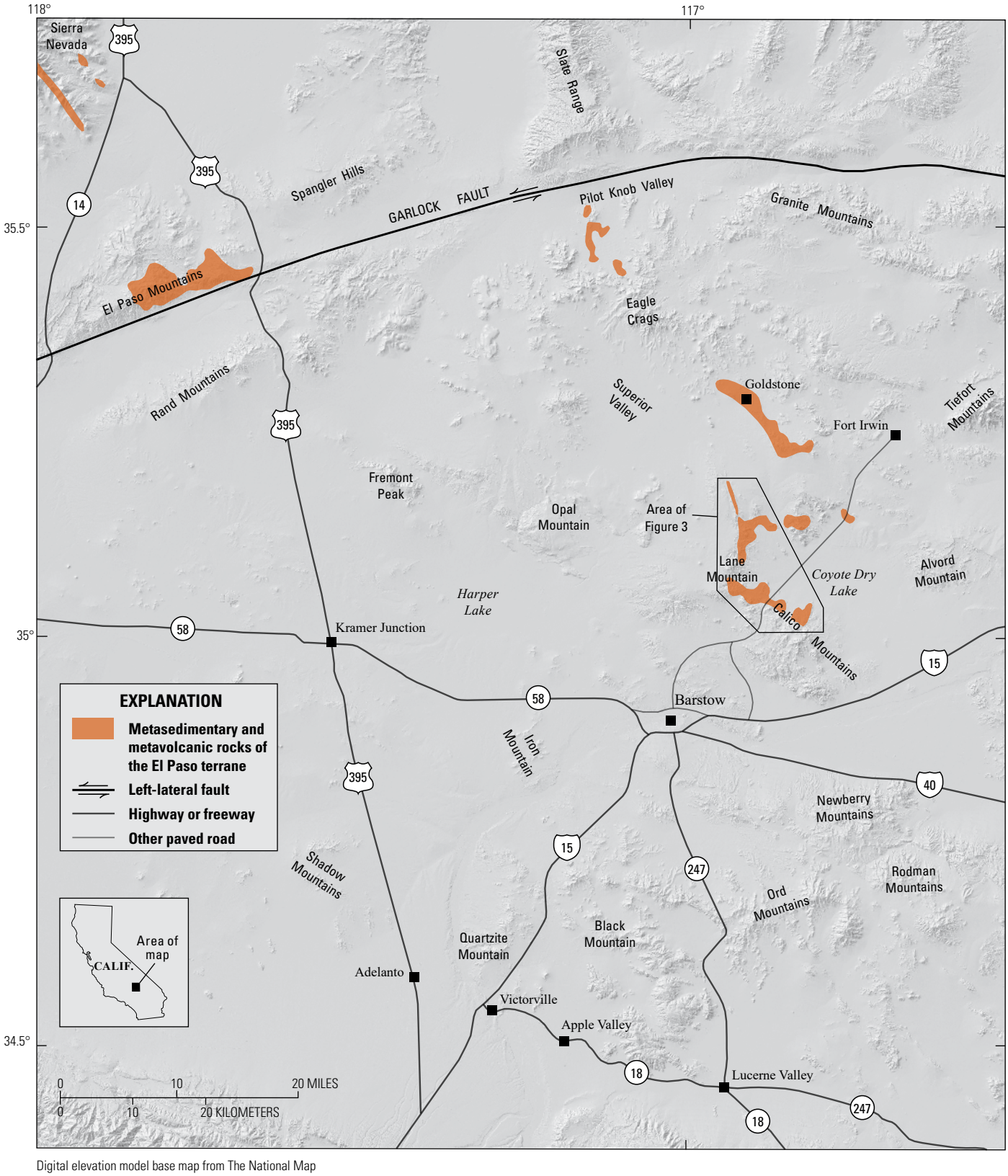

Digital elevation model base map from The National Map

Figure 1. Map of north-central Mojave Desert region showing outcrops of El Paso terrane (modified from Jennings and others, 1977) and location of report area (fig. 3). Outcrops of El Paso terrane extend ~30 kilometers northwest of the area shown (Saleeby and Dunne, 2015).

framework is well established, the tectonic relations of the El Paso terrane and the low-Sr_i plutonic belt are still not fully resolved.

To provide data for addressing this gap in understanding, the authors are conducting a multifaceted investigation of the Lane Mountain area that includes detailed geologic mapping, U-Pb zircon geochronology, Rb-Sr isotopic analysis, and geochemical analysis. Preliminary results of this investigation, focused primarily on the geologic mapping, were presented in several abstracts (Brown, 2016a, b, 2020; Brown and others, 2016, 2018). More recently, Stone and others (2019, 2021) presented geochronologic, isotopic, and geochemical data from igneous rocks in the area. Here we present geochronologic and

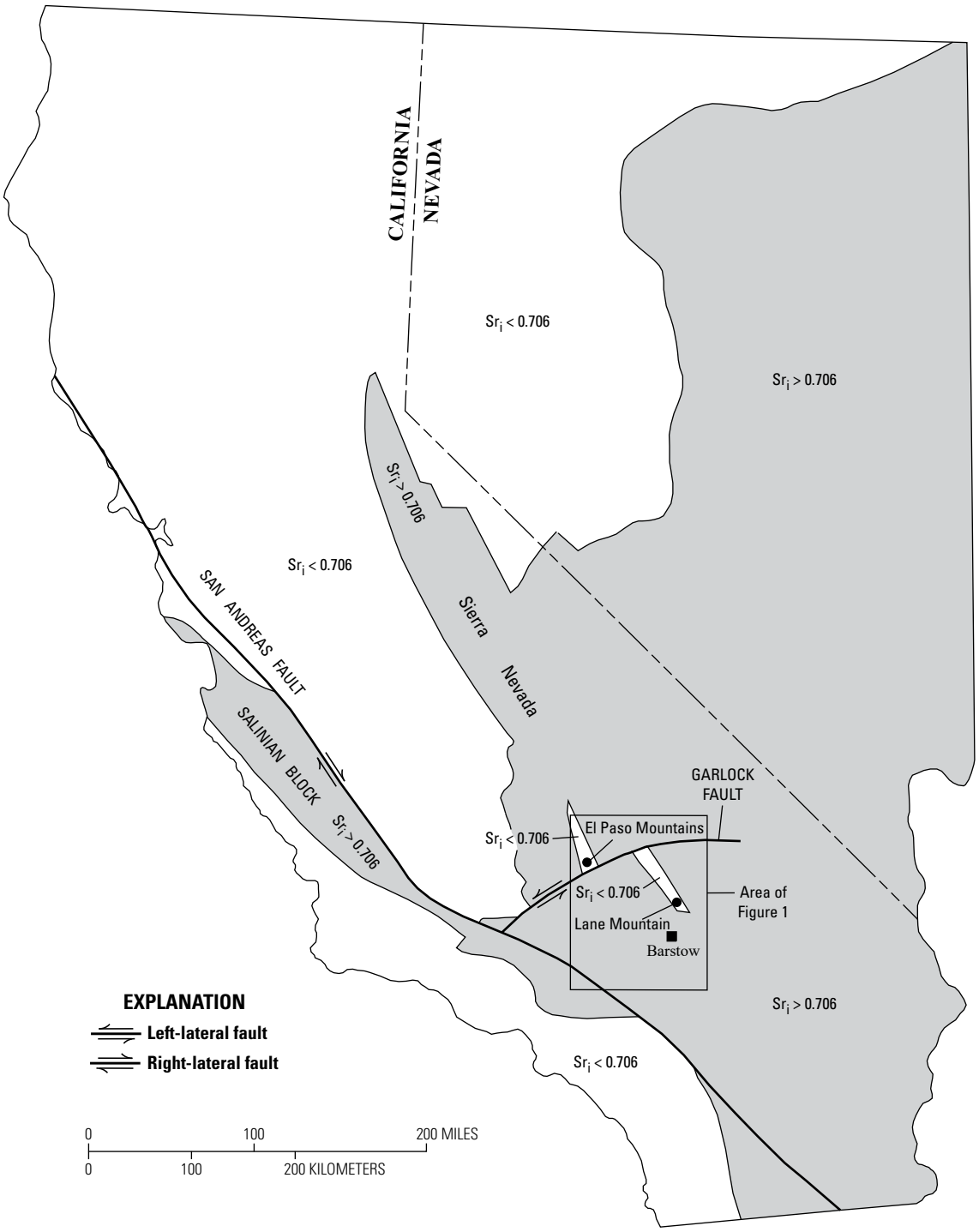

Figure 2. Map showing Sr_i = 0.706 isopleth in California and Nevada (modified from Kistler and Ross, 1990). Shaded areas have Sr_i >0.706. Note narrow, northwest-trending zone of Sr_i < 0.706 in El Paso Mountains–Lane Mountain area. Box shows area of figure 1.

geochemical data from the associated metasedimentary and related rocks to help clarify the stratigraphic and structural framework of the Lane Mountain area and contribute to a better general understanding of the El Paso terrane. Comma separated value files of the tabular data presented and discussed herein are available in a separate data release (Stone and others, 2023; https://doi.org/10.5066/P9G6YNEF).

Geographic Setting

The report area includes parts of the Lane Mountain, Williams Well, Paradise Range, and Coyote Lake 7.5-minute quadrangles, which together compose the area formerly covered by the Lane Mountain 15-minute quadrangle. The area (fig. 3) encompasses bedrock uplands that extend northward and southeastward from Lane Mountain, including the northern part of the Calico Mountains. These uplands drain eastward and northward into a broad, alluvial valley that includes Coyote Dry Lake, which is about 15 km east of Lane Mountain. Access to the area is provided by Fort Irwin Road and a network of unpaved roads shown on the topographic quadrangle maps.

Previous Investigations and Geologic Framework

The geology of the Lane Mountain 15-minute quadrangle was mapped by McCulloh (1952, 1960), who distinguished various units of pre-Cenozoic metamorphic and plutonic rocks and of Cenozoic volcanic and sedimentary rocks. Later analytical work added geochronologic, isotopic, and geochemical data that refined the framework of both the pre-Cenozoic and Cenozoic rocks (Burke and others, 1982; Miller and Sutter, 1982; Miller and Glazner, 1995; Miller and others, 1995; Singleton and Gans, 2008). A modified version of the map of McCulloh (1960) was published by Dibblee (2008).

A simplified version of McCulloh's (1960) mapping, together with updated age information derived from previous abstracts and reports by the authors (Brown and others, 2018; Stone and others, 2019, 2021) and from this report, is shown in figure 3. Four major lithologic assemblages are shown: (1) metamorphosed and deformed sedimentary and volcanic rocks of Paleozoic and Mesozoic age; (2) mostly mafic to intermediate-composition plutonic rocks of late Permian to Late Jurassic age; (3) felsic plutonic rocks of Late Cretaceous age; and (4) Cenozoic volcanic and sedimentary rocks that unconformably overlie the older rocks. The pre-Cretaceous plutonic rocks consist of a Permian to Triassic suite, which is confined to the western part of the study area, and a more extensive Late Jurassic suite (Stone and others, 2019, 2021). Some of the metamorphic rocks are intruded by the Permian to Triassic plutonic suite, but some are interpreted to be younger than that suite on the basis of detrital zircon ages presented herein. This relation complicates the geologic framework and indicates an intertwined history of sedimentation, magmatism, metamorphism, and deformation.

McCulloh (1960) divided the metasedimentary and metavolcanic rocks of the Lane Mountain area into four informally named formations (table 1). Most of the rocks were assigned to the Carbide formation (fig. 3), which McCulloh (1952) previously had called the Coyote group. As mapped by McCulloh (1960), the Carbide formation comprises a generally east-dipping sequence of 17 unnamed lithologic units that have a combined structural thickness of about 9 km (McCulloh, 1952, 1960; table 1). The dominant rock type is fine-grained, impure quartzite, but the sequence also includes pure quartzite, calcitic marble, dolomitic marble, siliceous hornfels, calc-silicate hornfels, metaconglomerate, and schist. Two units of dark metavolcanic rocks are also present, one at the base of the sequence and one near the middle. The great thickness of the Carbide formation is likely due in part to structural deformation, although no major repetition of the lithologic units is apparent.

The other three formations of McCulloh (1960) structurally overlie the lower part of the Carbide formation in the western part of the Lane Mountain area (fig. 3). The lowest of these, the Williams Well formation, is about 200 m thick and consists of quartzite, metaconglomerate, and marble. The overlying Starbright formation is about 300 m thick and consists of calcitic and dolomitic marble. The uppermost, Noble Well formation is about 1,800 m thick and consists primarily of hornfels, quartzite, and metaconglomerate. Large parts of the Noble Well formation were obliterated by the intrusion of Late Jurassic plutons. Rocks of all three formations had previously been assigned to the Starbright group of McCulloh (1952), and all three were mapped as fault bounded by McCulloh (1960). Geologic mapping by the authors has shown that the field relations of all three units are complex and should be reevaluated.

The metasedimentary and metavolcanic rocks in the Lane Mountain area are complexly deformed and commonly exhibit tight to isoclinal, small-scale folds, many of which have steeply plunging hinge lines. Original bedding and lamination, however, are commonly preserved. Petrographic data presented by McCulloh (1952) indicate mineralogical associations characteristic of greenschist- to amphibolite-grade metamorphism.

McCulloh (1952) interpreted all the metasedimentary rocks in the Lane Mountain area as Paleozoic on the basis of crinoid stems in marble of the informal Coyote group and fossil shell fragments identified as brachiopods in hornfels of the Starbright group. McCulloh (1960) assigned this same hornfels and the associated quartzite and conglomerate to the Noble Well formation, which he reinterpreted as Mesozoic on the basis of updated fossil identifications (appendix 1). McCulloh (1960) considered both the Carbide and Williams Well formations to be Paleozoic on the basis of meager fossil evidence (appendix 1) but did not assign any specific age to the Starbright formation, from which no fossils are known. Subsequently, Rich (1971) reported poorly preserved fusulinids from member 3 of the Coyote group (unit Pcmcg of McCulloh, 1960; table 1), which, if valid, would indicate a Pennsylvanian or Permian age. Except for shell fragments in the Noble Well formation, we have been unable to confirm the presence of fossils at any of the previously described localities, and our attempts to extract conodonts from several marble outcrops have been unsuccessful.

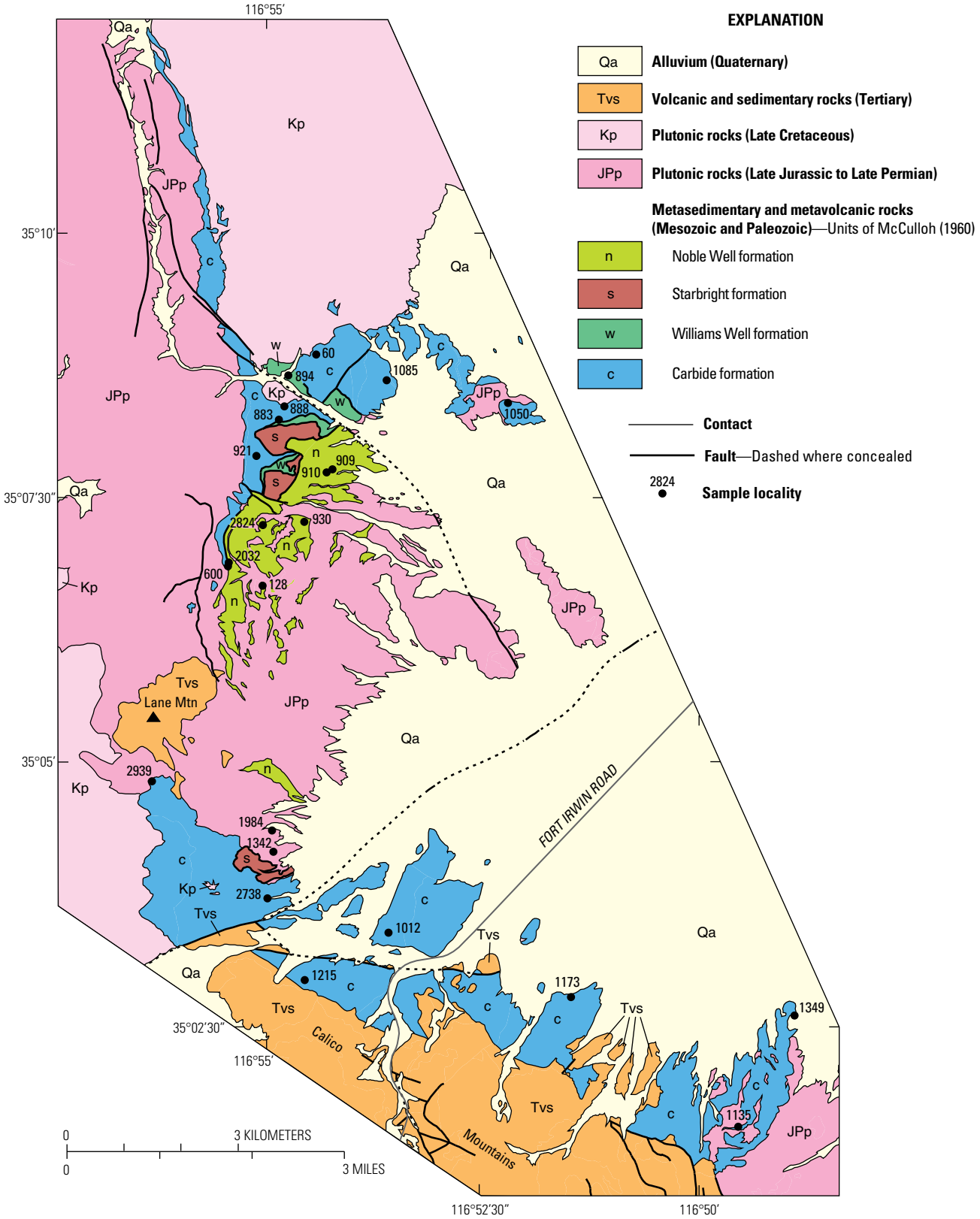

Figure 3. Map showing general geology of Lane Mountain area (modified from McCulloh, 1960) and locations of samples included in report. Note abbreviated sample numbers; see tables 2 and 3 for complete sample numbers.

Table 1. Metasedimentary and metavolcanic rock units of McCulloh (1960) in Lane Mountain area.

[Formation names, ages, map unit symbols, and lithologic descriptions are from McCulloh (1960); ages do not reflect new interpretations based on geochronologic data in this report. Thicknesses of units in the Carbide formation are from McCulloh (1952); other thicknesses are estimated from McCulloh (1960). Noble Well, Starbright, and Williams Well formations together are equivalent to Starbright group of McCulloh (1952); Carbide formation is equivalent to Coyote group of McCulloh (1952). See table 2 for complete sample numbers. --, no data.]

Map Unit	Lithology	Detrital Zircon Samples	Thickness (meters)
	Noble Well formation (Mesozoic)		
Mznw	Undifferentiated hornfels, feldspathic quartzite, pebble conglomerate, and marble	909, 910, 930	
MZnm	Marble (locally tactite)	--	[1]~2,000
Mznc	Meta-conglomerate and meta-arkose	128	
	Fault—Starbright formation (relative age uncertain)		
Usm	Marble and dolomite marble	--	~300
	Fault—Williams Well formation (Paleozoic)		
Pwu	Conglomerate, marble, and schist	--	
Pwm	Marble	--	[2]~200
Pwc	Pebble conglomerate, micaceous and feldspathic quartzite, and Ca-Mg silicate hornfels	894	
	Fault—Carbide formation (Paleozoic)		
Pcq_3	Quartzite and schist	--	
Pch_4	Wollastonite-diopside hornfels derived from siliceous dolomite	--	
Pcs_3	Biotite-muscovite-quartz schist	--	
Pch_3	Hornfels derived from impure dolomite or marl	--	[3]~400
Pcmb	Meta-basalt	--	
Pch_2	Hornfels derived from siliceous dolomite	--	
Pcs_2	Biotite-muscovite-quartz schist	--	
Pcu_1	Undifferentiated quartzite, schist, and rare marble	1135	~1,000
Pcq_2	Feldspathic quartzite, meta-arkose, biotite-muscovite-quartz, schist, and vitreous quartzite	1050, 1085, 1173	1,960
Pcma	Hornfels derived from andesitic flows	--	1,620
Pcs_1	Slightly schistose siltstone and shale	1012	
Pcm	Lenses and beds of siliceous marble	--	[4]230
Pch_1	Hornfels derived from sandy dolomite	60	
Pcmc	Recrystallized bedded chert	--	340
Pcmcg	Metamorphosed chert conglomerate	1215	590
Pcq_1	Feldspathic quartzite and schist with minor interbedded marble and hornfels	883, 888, 921, 2738	2,580
Pca	Amphibolite and biotite amphibolite derived from andesitic tuff	--	320

[1]Thickness refers to entire Noble Well formation.

[2] Thickness refers to entire Williams Well formation.

[3] Thickness refers to units Pcq_3 through Pcs_2.

[4] Thickness refers to units Pcs_1 through Pch_1.

Purpose and Scope

This study limits the depositional ages of selected metasedimentary rock units in the Lane Mountain area based on U-Pb dating of detrital zircons. Over the course of the study, 31 samples were processed for zircons, 23 of which were chosen for analysis. The other eight samples yielded either no zircons or too few to warrant analysis. Upon analysis, 17 of the 23 samples were confirmed to be metasedimentary rocks from which all or most of the dated zircons yielded chronologic data of potential value for constraining the depositional age and provenance. Of these 17 samples, 11 are from the Carbide formation, one is from the Williams Well formation, four are from the Noble Well formation, and one is from an unnamed quartzite unit not mapped by McCulloh (1960; tables 1, 2). One of the other six samples is a quartzite from the Carbide formation in which all the zircons were determined to be metamorphic, and the remaining five were ultimately interpreted to be of igneous rather than sedimentary origin (table 3). All 23 sample localities are shown on figure 3.

Table 2. Location and other information for the 17 detrital zircon samples included in this report

[Sample 16-LM-1342 is from a unit not mapped by McCulloh (1960). Ages, in mega-annum (Ma), are also shown in table 6; queried ages are based on youngest single zircons. Horizontal coordinate information is referenced to the North American Datum of 1927 (NAD27). --, no data]

Sample No.	Latitude (North) Longitude (West)	Formation	Unit	Lithology	Approximate Maximum Depositional Age
14-LM-60	35° 08' 51.1" 116° 54' 29.4"	Carbide	Pch_1	Medium-grained quartzite	224
14-LM-128	35° 06' 40.2" 116° 55' 05.0"	Noble Well	Mznc	Coarse-grained, granule-bearing metasandstone	194
15-LM-883	35° 08' 14.0" 116° 54' 54.2"	Carbide	Pcq_1	Metaconglomerate with clasts to 4 mm diameter	252
15-LM-888	35° 08' 21.6" 116° 54' 50.0"	Carbide	Pcq_1	Coarse-grained impure quartzite	939(?)
15-LM-894	35° 08' 39.3" 116° 54' 48.1"	Williams Well	Pwc	Metaconglomerate with clasts to 2 mm diameter	281
15-LM-909	35° 07' 46.3" 116° 54' 17.3"	Noble Well	Mznw	Metasandstone composed of calc-silicate minerals and biotite	214
15-LM-910	35° 07' 44.5" 116° 54' 20.6"	Noble Well	Mznw	Metasandstone like sample 909	192
15-LM-921	35° 07' 53.4" 116° 55' 09.7"	Carbide	Pcq_1	Fine grained quartzite	392(?)
15-LM-930	35° 07' 16.2" 116° 54' 35.8"	Noble Well	Mznw	Conglomeratic metasandstone	211
15-LM-1012	35° 03' 24.1" 116° 53'34.3"	Carbide	Pcs_1	Very fine-grained impure quartzite	238
15-LM-1050	35° 08' 25.1" 116° 52' 16.0"	Carbide	Pcq_2	Coarse-grained quartzite	1,027(?)
15-LM-1085	35° 08' 36.9" 116° 53' 40.6"	Carbide	Pcq_2	Medium-grained quartzite with abundant calc-silicate minerals	237
15-LM-1135	35° 01' 36.1" 116° 49' 30.7"	Carbide	Pcu_1	Coarse-grained quartzite with minor feldspar	1,036(?)
15-LM-1173	35° 02' 49.7" 116° 51' 28.0"	Carbide	Pcq_2	Fine-grained micaceous quartzite	230
16-LM-1215	35° 02' 57.0" 116° 54' 30.6"	Carbide	Pcmcg	Siliceous metaconglomerate	355(?)
16-LM-1342	35° 04' 09.0" 116° 54' 53.8"	--	--	Medium-grained quartzite	949(?)
17-LM-2738	35° 03' 42.9" 116° 54' 57.6"	Carbide	Pcq_1	Fine-grained quartzite	335(?)

Table 3. Location and other information for the six non-detrital zircon samples included in this report.

[Zircons from samples listed here are interpreted to have formed by metamorphic and magmatic processes. Ages, in mega-annum (Ma), are also shown in table 9. Ages apply to all samples of each group. Horizontal coordinate information is referenced to the North American Datum of 1927 (NAD27)]

Sample No.	Latitude (North) Longitude (West)	Descriptive Information	Approximate Magmatic or Metamorphic Age
		Quartzite Containing Metamorphic Zircons	
17-LM-1349	35° 02' 39.5" 116° 48' 53.6"	Coarse-grained quartzite in unit Pch_4 of the Carbide formation; zircons interpreted as metamorphic	150
		Albitized Igneous Rocks	
15-LM-600 17-LM-2032 18-LM-2939	35° 06' 50.6" 116° 55' 29.0" 35° 06' 51.9" 116° 55' 28.0" 35° 04' 48.1" 116° 56' 18.7"	Sheared, albite-rich rocks interpreted as altered igneous intrusions into unit Pcq1 of Carbide formation; zircons interpreted as magmatic	268
		Fine-grained Intrusive Rocks	
17-LM-1984 18-LM-2824	35° 04' 20.9" 116° 54' 55.2" 35° 07' 14.3" 116° 55' 03.8"	Fine-grained rocks interpreted as intrusive diorite to monzonite; zircons interpreted as magmatic. Sample 18-LM-2824 was mapped as part of Noble Well formation by McCulloh (1960); sample 17-LM-1984 is unmapped. A supplementary sample (17-LM-1984A) is from the same locality as sample 17-LM-1984	156

Methods

Zircon crystals were separated from ~0.5–2.5-kilogram (kg) samples at the U.S. Geological Survey (USGS) in Menlo Park, California. Most of the zircon U-Pb analyses were performed at California State University, Northridge (CSUN) using laser ablation sector field inductively coupled plasma mass spectrometry (LA-SF-ICPMS; table 4). Additional zircon U-Pb analyses were performed on the USGS sensitive high-resolution ion microprobe-reverse geometry (SHRIMP-RG) at Stanford University (table 5). Details of these methods are provided in appendix 2. Isoplot 4.15 software (Ludwig, 2012) was used to create graphic plots of the zircon data.

Geochemical analyses of the five samples of probable igneous origin were performed by AGAT Labs under contract to the USGS using wavelength-dispersive X-ray fluorescence (WDXRF) and inductively coupled plasma atomic emission spectroscopy-mass spectrometry (ICP-AES-MS).

All ages and age terms used in this report refer to the geologic time scale of Gradstein and others (2020).

Detrital Zircon Geochronology

This section presents the geochronological results for each of the 17 detrital zircon samples analyzed for this report. The zircon data were filtered to meet the following requirements: (1) age discordance (appendix 2) <15 percent positive or negative; (2) U concentration <5,000 ppm; and (3) U/Th ratio <10 (tables 4, 5 [available as supplemental files here: https://doi.org/10.3133/ofr20221115]). Ages of zircon grains not meeting these requirements are considered unreliable due to possible effects of post-depositional processes such as lead loss and metamorphism (Horie and others, 2006; Marcellos and Garver, 2010; Rubatto, 2017). The few zircon ages ≤160 mega-annum (Ma) not filtered out by the above criteria were eliminated on the geological basis that they are close to or less than the age of Late Jurassic plutonic rocks that intrude the metasedimentary units (Stone and others, 2019, 2021). Several anomalously young (~100 Ma and younger), highly discordant ages in some very fine-grained samples are ascribed to the analysis of minute apatite crystals mistaken for zircons.

The detrital zircon ages herein deemed acceptable on the basis of the above criteria were used to constrain the maximum depositional age of each sample. Three of the measures described by Dickinson and Gehrels (2009) for determining the maximum depositional age were employed: (1) YPP, the youngest age peak (based on two or more ages) on a probability density curve (figs. 4–6); (2) YC1σ[2+], the weighted mean age of the youngest cluster of two or more ages that overlap at one standard deviation (fig. 7); and (3) YSG, the youngest single grain age. All three ages are presented for each sample in table 6, with the preferred ages listed in table 2. In most cases, the preferred age is based on YC1σ[2+], and a more conservative (generally older) age is provided by YPP. The youngest single grain age, theoretically the closest to the true depositional age but also the most likely to be erroneously young, was used where considered geologically reasonable or

Table 6. Criteria for determining maximum depositional ages of detrital zircon samples included in this report.

[YPP, youngest age peak of two or more ages on probability density curve (figs. 4–6); YC1σ (n), weighted mean age of youngest cluster of two or more ages (n) overlapping at one standard deviation (1σ; fig. 7); YSG, youngest single age. --, no qualifying age peak or cluster available. Ages in mega-annum (Ma). YC1"sigma"(n) and YSG shown with 1"sigma" error.]

Sample	YPP	YC1σ(n)	YSG
14-LM-60	236	[2]224±8 (2)	220±6
14-LM-128	197	[2]194±3 (3)	193±2
15-LM-883	253	[2]252±7 (2)	250±7
[1]15-LM-888	1,163	1,142±38 (2)	[2]939±19
15-LM-894	281	[2]281±9 (2)	278±8
15-LM-909	242	[2]214±11 (2)	211±7
15-LM-910	192	[2]192±6 (2)	192±4
15-LM-921	447	445±16 (2)	[2]392±14
15-LM-930	217	[2]211±3 (11)	173±4
15-LM-1012	244	[2]238±5 (5)	223±7
15-LM-1050	1,854	1,655±29 (3)	[2]1,027±21
15-LM-1085	270	[2]237±6 (3)	215±5
15-LM-1135	1,835	1,830±17 (7)	[2]1,036±39
15-LM-1173	255	[2]230±11 (2)	227±8
16-LM-1215	793	769±18 (2)	[2]355±5
16-LM-1342	1,818	1,702±39 (8)	[2]949±24
18-LM-2738	--	--	[2]335±9

[1]Combined ICPMS and SHRIMP analyses (sample 15-LM-888).

[2]Preferred age.

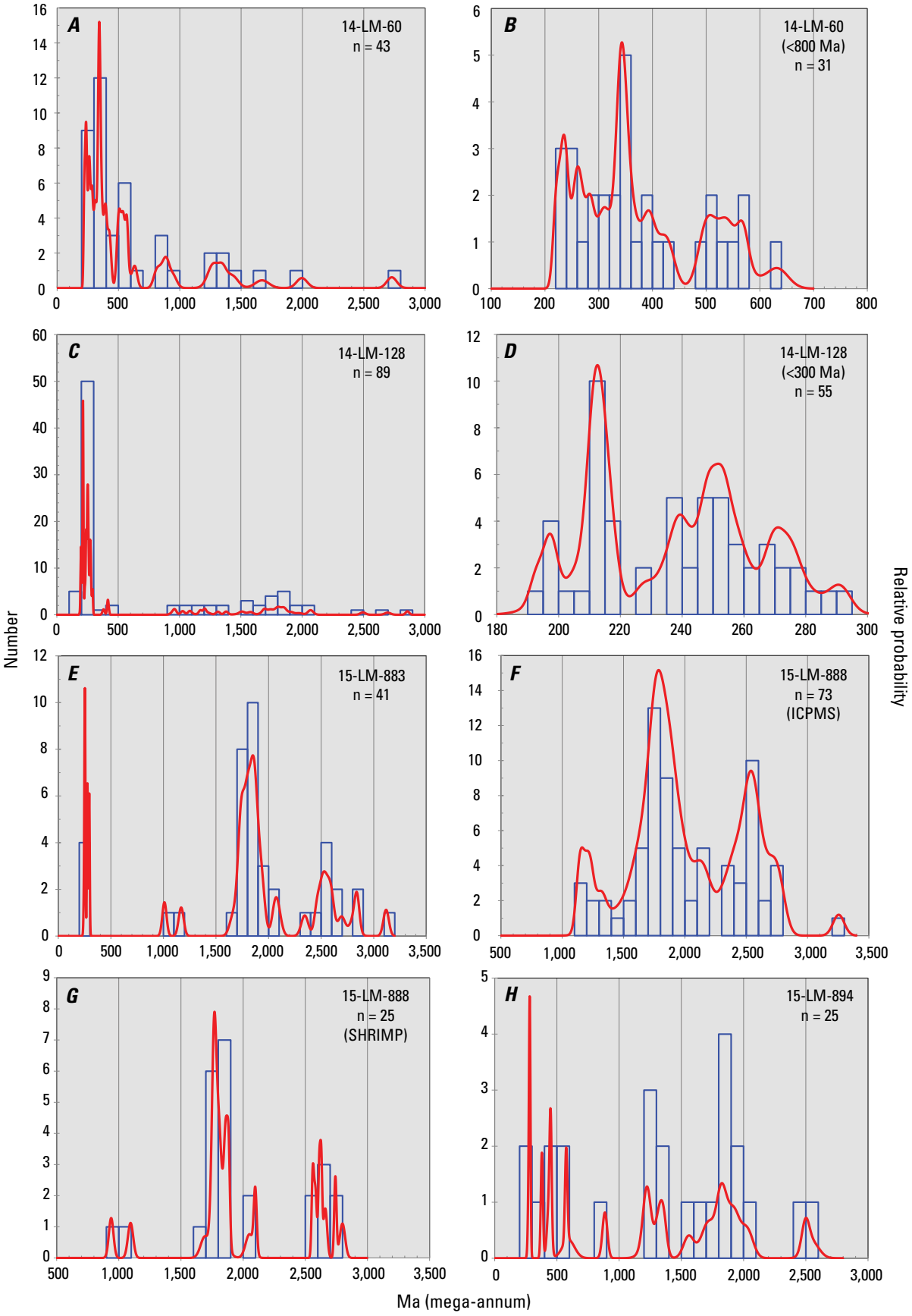

Figure 4. Probability density curves (red) and histograms (blue) of acceptable detrital zircon ages from samples 14-LM-60 (*A*, *B*), 14-LM-128 (*C*, *D*), 15-LM-883 (*E*), 15-LM-888 (*F*, *G*), and 15-LM-894 (*H*). Left vertical axis shows number of grains analyzed from each sample; right vertical axis shows relative probability. Plots were created using Isoplot 4.15 (Ludwig, 2012) from data in tables 4 and 5 (available as supplemental files here: https://doi.org/10.3133/ofr20221115).

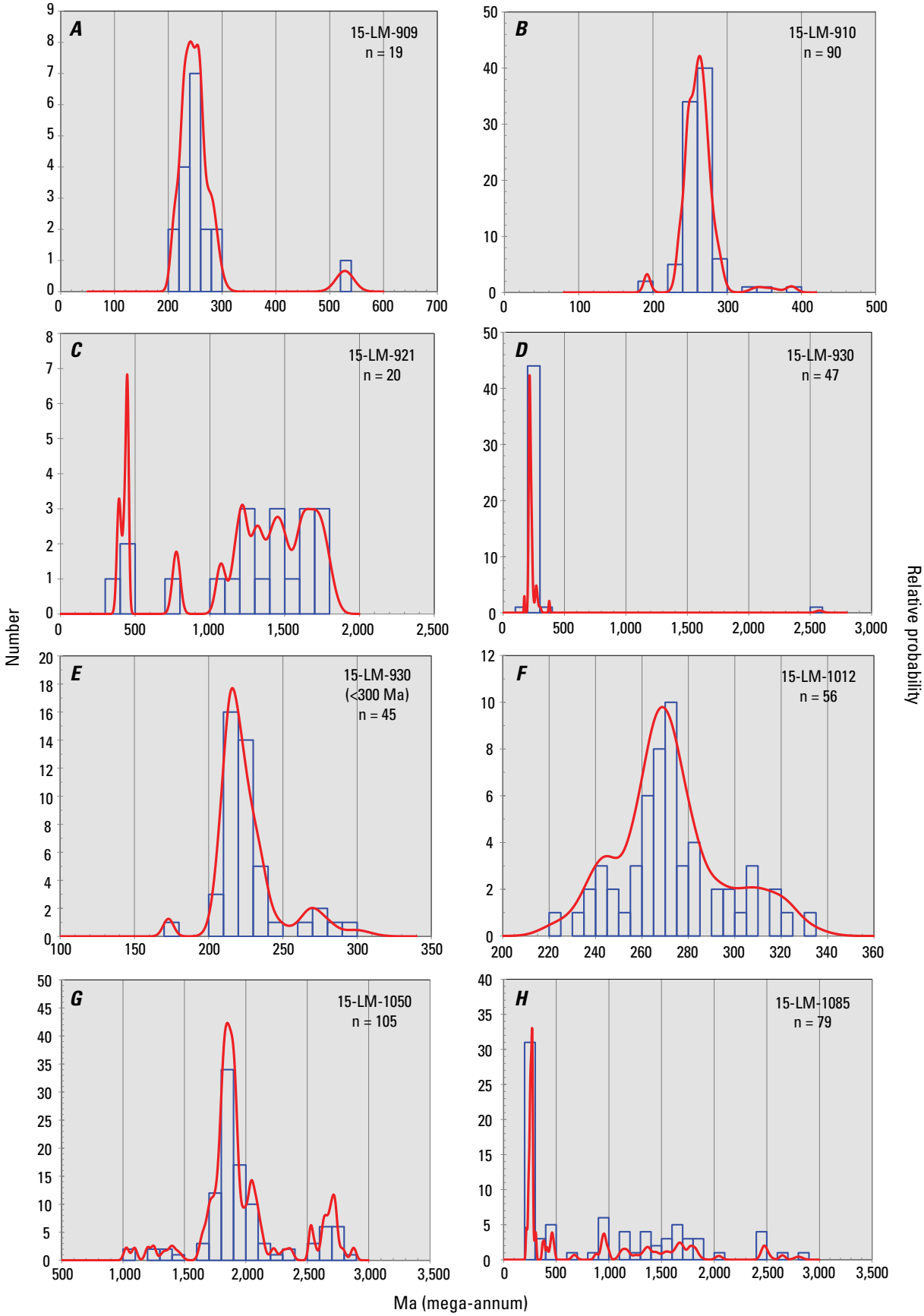

Figure 5. Probability density curves (red) and histograms (blue) of acceptable detrital zircon ages from samples 15-LM-909 (*A*), 15-LM-910 (*B*), 15-LM-921 (*C*), 15-LM-930 (D, *E*), 15-LM-1012 (*F*), 15-LM-1050 (*G*), and 15-LM-1085 (*H*). Left vertical axis shows number of grains analyzed from each sample; right vertical axis shows relative probability. Plots were created using Isoplot 4.15 (Ludwig, 2012) from data in table 4 (available as supplemental file here: https://doi.org/10.3133/ofr20221115).

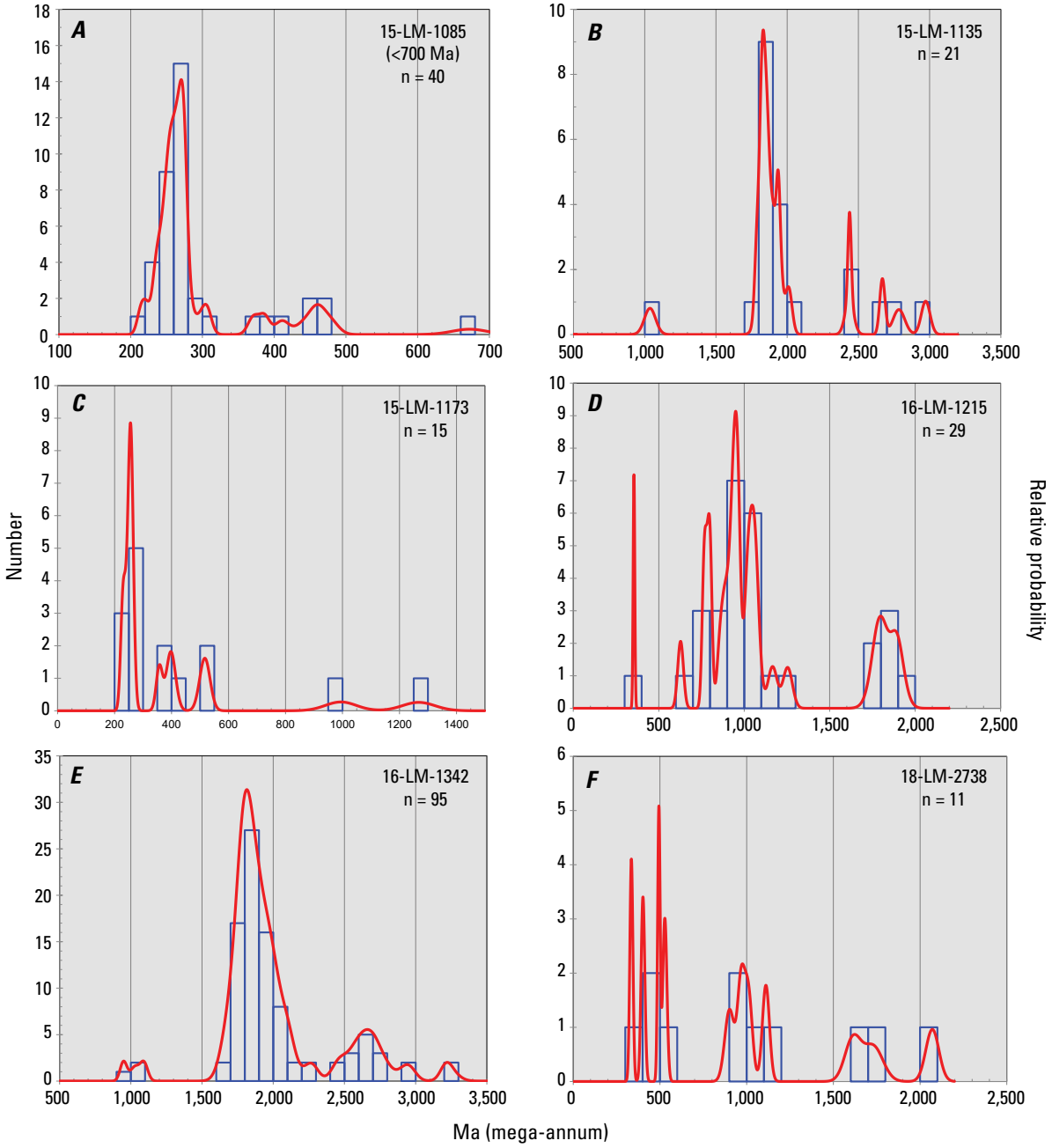

Figure 6. Probability density curves (red) and histograms (blue) of acceptable detrital zircon ages from samples 15-LM-1085 (*A*), 15-LM-1135 (*B*), 15-LM-1173 (*C*), 16-LM-1215 (*D*), 16-LM-1342 (*E*), and 18-LM-2738 (*F*). Left vertical axis shows number of grains analyzed from each sample; right vertical axis shows relative probability. Plots were created using Isoplot 4.15 (Ludwig, 2012) from data in tables 4 and 5 (available as supplemental files here: https://doi.org/10.3133/ofr20221115).

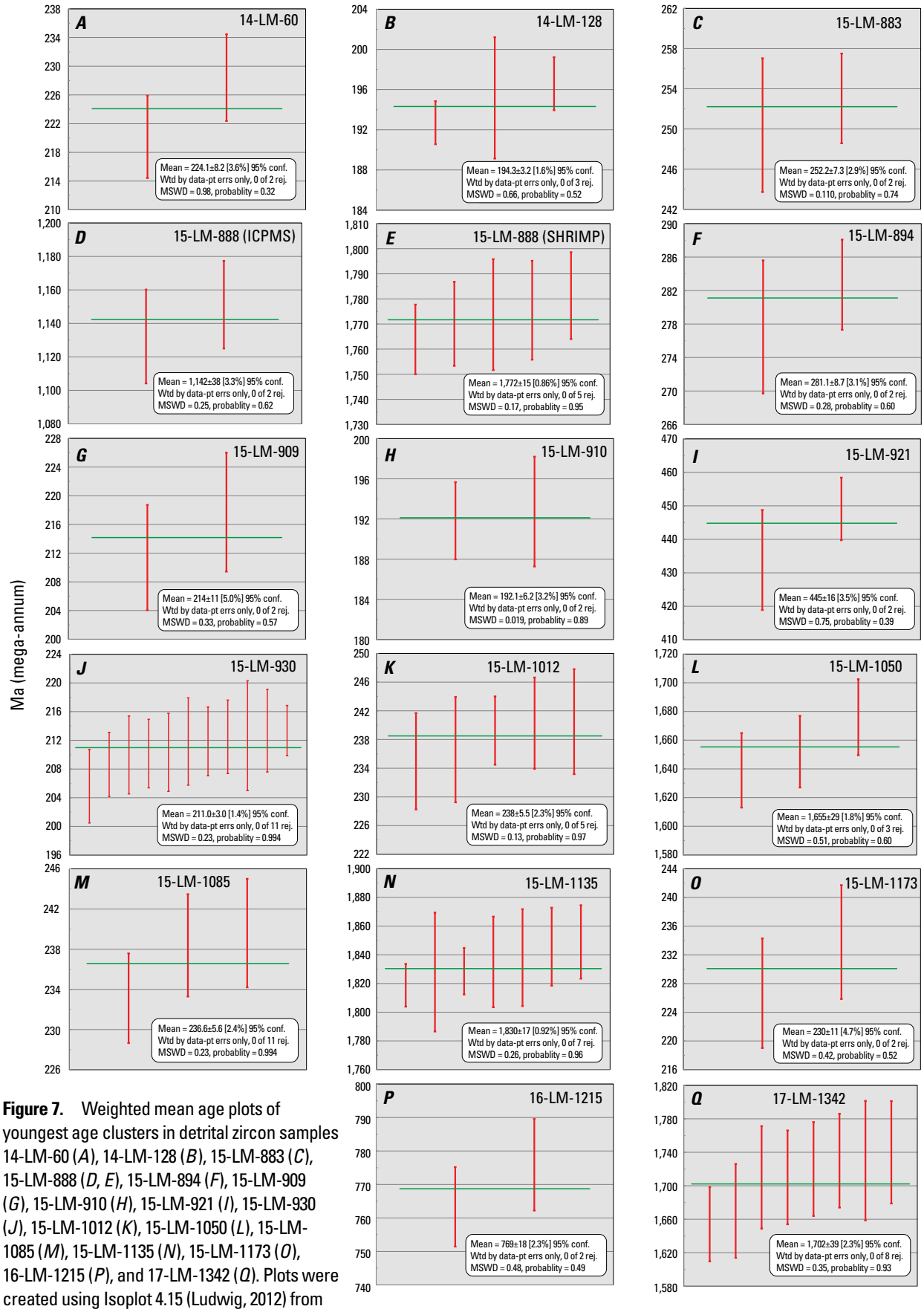

Figure 7. Weighted mean age plots of youngest age clusters in detrital zircon samples 14-LM-60 (*A*), 14-LM-128 (*B*), 15-LM-883 (*C*), 15-LM-888 (*D*, *E*), 15-LM-894 (*F*), 15-LM-909 (*G*), 15-LM-910 (*H*), 15-LM-921 (*I*), 15-LM-930 (*J*), 15-LM-1012 (*K*), 15-LM-1050 (*L*), 15-LM-1085 (*M*), 15-LM-1135 (*N*), 15-LM-1173 (*O*), 16-LM-1215 (*P*), and 17-LM-1342 (*Q*). Plots were created using Isoplot 4.15 (Ludwig, 2012) from data in tables 4 and 5 (available as supplemental files here: https://doi.org/10.3133/ofr20221115). Vertical red bars represent individual zircon ages with 1σ error; horizontal green lines are weighted mean ages calculated by Isoplot. Ma, mega-annum; MSWD, Mean Squared Weighted Deviation.

where neither of the other methods could be used. All maximum depositional ages based on YSG are queried.

The maximum depositional ages reported here are based on the presumption that the acceptable ages in the Lane Mountain detrital zircon dataset did not result from extreme post-depositional lead loss, which can cause complete resetting of the U-Pb systematics of detrital zircon crystals in metasedimentary rocks (Reimink and others, 2016; Clemens-Knott and Gevedon, 2022). This presumption is especially important for the interpretation of Triassic to Early Jurassic zircon ages in certain units (table 2) as valid indicators of post-Paleozoic deposition. Although the possibility that these ages instead resulted from extreme post-depositional lead loss cannot be entirely discounted, two lines of reasoning provide grounds for indicating that the Late Triassic to Early Jurassic maximum depositional ages determined for at least one unit, the Noble Well formation (table 2), are valid. First, these ages are consistent with the paleontologically constrained age of the Noble Well formation (appendix 1). Second, there is no independent evidence of Late Triassic to Early Jurassic magmatic or hydrothermal activity in the Lane Mountain area that could have driven a major lead-loss event of that age (Stone and others, 2019, 2021). On the basis of this evidence, the presumption that the detrital zircon ages reported here did not result from extreme post-depositional lead loss is provisionally considered to be valid, with the recognition that future studies could prove otherwise.

The following is a sample-by-sample description of the geochronological results, organized by formation and unit of McCulloh (1960). All analyses were conducted by ICP-AES-MS, except as noted in the following sections.

Carbide Formation

The 11 samples from the Carbide formation are from six different units and are described from lowest to highest within the lithologic sequence (table 1).

Unit Pcq_1

Unit Pcq_1, composed primarily of fine-grained, impure quartzite, is the structurally lowest metasedimentary unit of the Carbide formation. It overlies dark metavolcanic rocks assigned to the lowermost unit, unit Pca (table 1), the base of which is faulted against, and locally intruded by, Permian to Triassic plutonic rocks (Stone and others, 2021). South of Lane Mountain, as mapped by McCulloh (1960), unit Pcq_1 is >2,500 m thick and overlain by successive units of the Carbide formation, whereas to the north it is only ~400 m thick and overlain by rocks assigned to the Williams Well formation (fig. 3). Detrital zircon sample 18-LM-2738 is from the thick southern sequence and samples 15-LM-883, 15-LM-888, and 15-LM-921 are from the thinner, northern sequence.

Sample 15-LM-921

Sample 15-LM-921, the structurally lowest reported here, is from a sequence of fine-grained quartzite that is light gray on fresh surfaces and typically weathers light reddish gray. Mapping by the authors indicates that this sequence constitutes a discrete subunit of unit Pcq_1.

The sparse zircons from this sample are very small and yielded 20 acceptable ages (table 4). Of these, 16 are Paleoproterozoic to Mesoproterozoic (~1,790–1,074 Ma) and four are Neoproterozoic to Paleozoic (~776–392 Ma), with age peaks at ~1,500 and 447 Ma (fig. 5*C*). The maximum depositional age is questionably interpreted as ~392 Ma (Devonian) on the basis of the youngest single grain (YSG; table 6). An older, two-age cluster yields a more conservative maximum depositional age of ~445 Ma (YC1σ[2+]; fig. 7*I*, table 6).

Sample 15-LM-888

Sample 15-LM-888 is from a medium- to coarse-grained, impure quartzite bed about 300 m below the contact mapped by McCulloh (1960) between unit Pcq_1 and the overlying Williams Well formation (McCulloh, 1960). ICP-AES-MS analysis of zircons from this sample yielded 73 acceptable ages (table 4), all of which are Mesoproterozoic and older with an age range of ~3,254–1,132 Ma with prominent age peaks at ~2,538, 1,787, and 1,163 Ma (fig. 4*F*). A supplementary SHRIMP analysis yielded 25 acceptable ages with a range of ~2,799–939 Ma (table 5). The age distribution resembles that of the ICP-AES-MS analysis, with major peaks at ~2,620 and 1,770 Ma and two younger grains at ~1,095 and 939 Ma (fig. 4*G*).

The youngest, two-age cluster from the ICP-AES-MS analysis yields a weighted mean age of ~1,142 Ma (YC1σ[2+]; fig. 7*D*, table 6), but the maximum depositional age is questionably interpreted as ~939 Ma on the basis of the youngest single grain in the SHRIMP analysis (YSG; table 6). The youngest, five-age cluster from the SHRIMP analysis yields a weighted mean age of ~1,772 Ma (YC1σ[2+]; fig. 7*E*).

Sample 15-LM-883

Sample 15-LM-883 is from a bed of conglomeratic quartzite about 50 m below the contact mapped by McCulloh (1960), between unit Pcq_1 and the overlying Williams Well formation (fig. 3). Zircons from this sample yielded 41 acceptable ages (table 4), all but six of which are Paleoproterozoic and older with an age range of ~3,118–1,664 Ma and major peaks at ~2,530 and 1,850 Ma (fig. 4*E*). Two Mesoproterozoic grains at ~1,168 and 1,009 Ma are also present. The other four grains are much younger with early Permian to Early Triassic ages of ~294, 276, 253, and 250 Ma, defining a general peak at ~270 Ma. The small cluster defined by the two youngest ages indicates a maximum depositional age of ~252 Ma (YC1σ[2+]; fig. 7*C*, table 6) at the Permian and Triassic boundary.

Sample 18-LM-2738

Sample 18-LM-2738 is from a massive bed of very fine grained, light-brown-weathering, impure quartzite typical of the southern outcrop area of unit Pcq_1. Although this sample yielded about 100 zircons, most were so small that only 12 grains could

be successfully mounted and analyzed during two separate ICP-AES-MS runs. Eleven of these yielded acceptable ages with a range of ~2,071–335 Ma (table 4). These meager data define no useful age peaks (fig. 6*F*) or clusters, so the maximum depositional age is questionably interpreted as ~335 Ma (Mississippian) on the basis of the youngest single grain (YSG; table 6).

Unit Pcmcg

As mapped by McCulloh (1960), the chert-pebble metaconglomerate of unit Pcmcg overlies unit Pcq_1 in the southern part of the Lane Mountain area but does not extend farther north. Detrital zircons were recovered from a single sample, 16-LM-1215, in this unit.

Sample 16-LM-1215

Sample 16-LM-1215 was collected at the summit of a prominent hill near the southwest outcrop limit of unit Pcmcg, where it is overlain by or faulted against Miocene volcanic rocks (McCulloh, 1960; fig. 3). The sample consisted of loose monolithologic fragments because no true outcrop was available.

Zircons from sample 16-LM-1215 yielded 29 acceptable ages (table 4), 22 of which are Mesoproterozoic to Neoproterozoic (~1,254–628 Ma) with peaks at ~1,048, 950, and 793 Ma, and six of which are Paleoproterozoic (~1,906–1,785 Ma) with a peak at ~1,800 Ma (fig. 6*D*). The only younger age is ~355 Ma (Mississippian), which is questionably interpreted as the maximum depositional age (YSG; table 6). The youngest two-age cluster has a weighted mean age of ~769 Ma (YC1σ[2+]; fig. 7*P*, table 6).

Units Pch_1, Pcm, and Pcs_1

McCulloh (1960) divided an assemblage of mixed siliciclastic and carbonate rocks, recognized in both the northern and southern parts of the Lane Mountain area, into the three related map units Pch_1, Pcm, and Pcs_1 (table 1). This assemblage, which is ~230 m thick, yielded two samples from which detrital zircons were extracted: 14-LM-60 from the lower part of the sequence and 15-LM-1012 from the middle part.

Sample 14-LM-60

Sample 14-LM-60 is from a quartzite bed associated with metamorphosed carbonate rocks in unit Pch_1 of McCulloh (1960) in the northern part of the Lane Mountain area (fig. 3). Zircons from this sample yielded 43 acceptable ages (table 4). These include eight Mesoproterozoic and older ages (~2,728–1,258 Ma) with no prominent peaks and 35 Neoproterozoic to Triassic ages with a range of ~940–220 Ma and peaks at ~885, 560–500, 344, and 236 Ma (fig. 4*A*, *B*). The maximum depositional age is interpreted as ~224 Ma (Late Triassic) on the basis of a cluster of the two youngest ages (YC1σ[2+]; fig. 7*A*, table 6), with the youngest peak at ~236 Ma (YPP) providing a more conservative alternative.

Sample 15-LM-1012

Sample 15-LM-1012 is from fine-grained quartzite in unit Pcs_1 of McCulloh (1960) in the southwestern part of the Lane Mountain area (fig. 3). The sample locality is on the northwest side of a prominent northeast-trending ridge adjacent to Fort Irwin Road, structurally below a major zone of calcitic marble (unit Pcm).

Zircons from sample 15-LM-1012 yielded 56 acceptable ages ranging from ~330 to 223 Ma (table 4). The data define a major age peak at ~269 Ma and a subsidiary peak at ~244 Ma that reflects the presence of nine ages between ~252 and 235 Ma (fig. 5*F*). A tight cluster of five ages between ~240 and 235 Ma indicates a Middle Triassic maximum depositional age of ~238 Ma (YC1σ[2+]; fig. 7*K*, table 6).

Unit Pcq_2

Unit Pcq_2 is a thick sequence of quartzitic rocks mapped by McCulloh (1960) in both the northern and southern parts of the Lane Mountain area. This unit, which is nearly 2,000 m thick, overlies a unit of dark metavolcanic rocks (Pcma) that marks the approximate middle of the Carbide formation. Three samples from rocks included in unit Pcq_2 yielded detrital zircons: 15-LM-1085 and 15-LM-1050 in the northern part of the area, and 15-LM-1173 in the southern part (fig. 3). Samples 15-LM-1085 and 15-LM-1173 probably represent about the same structural level within unit Pcq_2, whereas sample 15-LM-1050 is structurally higher.

Sample 15-LM-1085

Sample 15-LM-1085 is from a medium-grained, impure quartzite that contains abundant calc-silicate metamorphic minerals. Zircons from this sample yielded 79 acceptable ages (table 4), 40 of which are Neoproterozoic and older (~2,801–672 Ma) with no major peaks (fig. 5*H*). The other 39 ages range from Ordovician to Late Triassic (~479–215 Ma), with a minor peak at ~460 Ma and a major peak at ~271 Ma (figs. 5*H*, 6*A*). A cluster of three ages between ~240 and 233 Ma indicates a Middle Triassic maximum depositional age of ~237 Ma (YC1σ[2+]; fig. 7*M*, table 6).

Sample 15-LM-1173

Sample 15-LM-1173, which is from a fine-grained quartzite, contained sparse, very small zircons. The 15 zircons that were analyzed all yielded acceptable ages ranging from Mesoproterozoic to Triassic (~1,267–227 Ma; table 4). Thirteen grains are ~519 Ma and younger, of which the youngest eight are between ~263 and 227 Ma and produce a peak at ~255 Ma (fig. 6*C*). The two youngest ages in this group define a cluster that indicates a maximum depositional age of ~230 Ma (YC1σ[2+]; fig. 7*O*, table 6), close to that of sample 15-LM-1085.

Sample 15-LM-1050

Sample 15-LM-1050 is from a light-gray, coarse-grained orthoquartzite that forms a prominent hill near the northeastern margin of the Lane Mountain study area (fig. 3). This quartzite is

lithologically distinct from the finer grained, impure quartzites of samples 15-LM-1085 and 15-LM-1173 and is separated from the rest of unit Pcq_2 by Late Jurassic plutonic rocks (Stone and others, 2021). The quartzite is associated with laminated calc-hornfels and minor marble.

Sample 15-LM-1050 yielded abundant zircons, many of them rounded. The analysis produced 105 acceptable ages, 98 of which range from ~2,877 to 1,639 Ma (table 4) with prominent peaks at ~2,710 and 1,850 Ma (fig. 5*G*). Seven Mesoproterozoic ages range from ~1,448 to 1,027 Ma, the youngest of which is questionably interpreted as the maximum depositional age (YSG; table 6). The youngest three-age cluster has a weighted mean age of ~1,655 Ma (YC1σ[2+]; fig. 7*L*, table 6).

The contrasts in lithology, associated rock assemblages, and zircon age distribution of sample 15-LM-1050 relative to those of samples 15-LM-1085 and 15-LM-1173 lead to the conclusion that this sample represents a separate lithologic unit not differentiated by McCulloh (1960).

Unit Pcu_1

Unit Pcu_1 of McCulloh (1960) is a heterogenous assemblage of metamorphosed siliciclastic rocks and marble in the upper (eastern) part of the Carbide formation. These rocks are heavily intruded by Late Jurassic plutonic rocks (Stone and others, 2021). A volumetrically minor but characteristic rock type in the metasedimentary assemblage is light-gray, pure to nearly pure quartzite, including a prominent bed near the structural top of unit Pcu_1. A sample from this bed (15-LM-1135) yielded detrital zircons as well as zircons of probable metamorphic origin, as described below.

Sample 15-LM-1135

Sample 15-LM-1135 is a massive, light-gray, vitreous quartzite that is pure except for minor feldspar forming irregular patches interstitial to the dominant quartz. The rock is highly recrystallized, and the origin of the feldspar is uncertain.

Numerous zircons were extracted from sample 15-LM-1135, 36 of which were analyzed on the SHRIMP; no ICP-AES-MS analysis of this sample was performed. Of these, 22 yielded acceptable detrital ages, 20 of which range from ~2,972 to 1,787 Ma (table 5) with a minor peak at ~2,438 Ma and a prominent peak at ~1,835 Ma (fig. 6*B*). The youngest single age of ~1,036 Ma is questionably interpreted as the maximum depositional age (YSG; table 6); the youngest seven-age cluster has a weighted mean age of ~1,830 Ma (YC1σ[2+]; fig. 7*N*, table 6).

Sample 15-LM-1135 also yielded a younger group of nine zircons that range in age from ~158 to 145 Ma with a peak at ~150 Ma. These zircons, which have elevated U/Th ratios that range from 4 to 10, are interpreted to have formed by post-depositional metamorphism related to intrusion of the coeval Late Jurassic plutonic rocks.

In addition to zircons, sample 15-LM-1135 also yielded abundant, rounded grains of detrital titanite (sphene) that were not analyzed but are presumed to be Precambrian on the basis of their morphology.

Williams Well Formation

The single detrital zircon sample (15-LM-894) from the Williams Well formation is from unit Pwc (McCulloh, 1960), which is characterized primarily by metaconglomerate and arkosic quartzite (table 1). The sample locality is in a well exposed, south-dipping sequence of interbedded metaconglomerate, quartzite, and minor marble on the northeast side of a major wash (fig. 3). This sequence, although mapped as part of the Williams Well formation by McCulloh (1960), is not demonstrably overlain by rocks of the Starbright formation, which is only exposed southwest of the wash.

Sample 15-LM-894

Sample 15-LM-894 is from a bed of dark-gray metaconglomerate composed of ~50 percent angular to subrounded clasts in a dark, sandy matrix. Clasts include fine-grained quartzite, coarse-grained polycrystalline quartz, and large plagioclase grains >1 mm across. Zircons from this sample yielded 25 acceptable ages ranging from ~2,550 to 278 Ma (table 4). Of these ages, 17 are Mesoproterozoic or older with a small peak at ~2,500 Ma and larger peaks at ~1,830 and 1,220 Ma (fig. 4*H*). The other eight acceptable ages are Neoproterozoic to late Paleozoic between ~886 and 278 Ma. The two youngest ages form a peak and cluster that indicate an early Permian maximum depositional age of ~281 Ma (YC1σ[2+]; fig. 7*F*, table 6).

Noble Well Formation

Three of the four detrital zircon samples from the Noble Well formation (15-LM-909, 15-LM-910, and 15-LM-930) are from rocks mapped as unit Mznw (undifferentiated hornfels, feldspathic quartzite, pebble metaconglomerate, and marble) by McCulloh (1960; table 1). The other sample (14-LM-128) is from unit Mznc, which is characterized by metaconglomerate and meta-arkose. McCulloh (1960) mapped a fault between the northern part of the Noble Well formation, which contains samples 15-LM-909 and 15-LM-910, and the southern part, which contains samples 14-LM-128 and 15-LM-930 (fig. 3). Mapping by the authors indicates that this fault is more extensive and significant than implied by McCulloh (1960) and separates two lithologically distinct units: fine-grained quartzite and metamorphosed carbonate rocks to the north in contrast to hornfels and metaconglomerate to the south. The two sets of zircon samples are described sequentially below.

Samples 14-LM-128 and 15-LM-930

Sample 14-LM-128 is from a coarse-grained metasandstone that contains scattered clasts to 5 mm across, many of which are

polycrystalline quartz. The rock is highly recrystallized, and the original sedimentary texture is not well preserved.

Zircons from sample 14-LM-128 yielded 89 acceptable ages ranging from ~2,858 to 193 Ma (table 4). Of these, 31 are Neoproterozoic or older (~2,858–948 Ma) with a minor peak at ~1,850 Ma, and 58 are Devonian to Jurassic (~420–193 Ma) with a minor peak at ~420 Ma and prominent peaks at ~252 and 212 Ma; a detailed plot of ages <300 Ma reveals additional peaks at ~270, 240, and 198 Ma (fig. 4*C*, *D*). The three youngest ages form a cluster that indicates an Early Jurassic maximum depositional age of ~194 Ma (YC1σ[2+]; fig. 7*B*, table 6).

Sample 15-LM-930 is from a dark-gray metaconglomerate bed containing quartzite pebbles and large plagioclase grains in an impure quartzite matrix. Many of the pebbles are tectonically stretched.

Zircons from sample 15-LM-930 yielded 47 acceptable ages (table 4), 45 of which range from ~376 to 206 Ma and define a major Late Triassic peak at ~217 Ma (fig. 5*D*, *E*). The other two ages are Archean (~2,575 Ma) and Middle Jurassic (~173 Ma). The Jurassic age shows no obvious signs of lead loss or metamorphism and could represent the maximum depositional age of the sample. However, an age that young would be inconsistent with other evidence pertaining to the regional correlation of the Noble Well formation (see "Discussion" section) and would thus require stronger evidence to be confidently supported. For this reason, the maximum depositional age of the sample is here considered to be ~211 Ma on the basis of a robust cluster of 11 ages between ~213 and 206 Ma (YC1σ[2+]; fig. 7*J*, table 6).

Samples 15-LM-909 and 15-LM-910

Sample 15-LM-909 is from a bed of medium-gray, thoroughly metamorphosed calcareous sandstone composed primarily of calc-silicate minerals and biotite with little or no remnant quartz. This bed overlies a thick bed of brown dolomitic marble.

Zircons from sample 15-LM-909 yielded 19 acceptable ages with a range of ~528–211 Ma and a peak at ~242 Ma (table 4, fig. 5*A*). The two youngest ages form a cluster that indicates a Late Triassic maximum depositional age of ~214 Ma (YC1σ[2+]; fig. 7*G*, table 6), comparable to that of sample 15-LM-930. An older, more robust cluster of three ages has a weighted mean age of ~229 Ma (YC1σ[2+]), which is considered the oldest possible depositional age of the sample. Several zircons in this sample were found to have Late Jurassic rims during the analysis, indicating an episode of secondary zircon growth related to the intrusion of nearby plutonic rocks of similar age (Stone and others, 2019, 2021).

Sample 15-LM-910 was collected to supplement the sparse detrital zircon data that had been obtained from nearby sample 15-LM-909. Both samples are lithologically similar and are interpreted to represent a similar stratigraphic position above the same bed of brown dolomitic marble.

Zircons from sample 15-LM-910 were analyzed in two separate ICP-AES-MS runs that yielded a total of 90 acceptable ages ranging from ~387 to 192 Ma (table 4). Of these ages, 85 are between ~290 and 234 Ma, with a late middle Permian peak at ~264 Ma (fig. 5*B*) and a weighted mean age of ~235 Ma (YC1σ[2+]) for the five youngest ages in this part of the dataset. These data indicate a depositional age no older than earliest Middle Triassic. However, the two youngest ages in the sample comprise a cluster that is here interpreted to indicate a much younger, Early Jurassic maximum depositional age of ~192 Ma (YC1σ[2+]; fig. 7*H*, table 6), comparable to that of sample 14-LM-128.

Unnamed Quartzite

Sample 16-LM-1342

The remaining detrital zircon sample (16-LM-1342) is from a small quartzite outcrop not differentiated from the surrounding, intrusive diorite by McCulloh (1960) in the southwestern part of the Lane Mountain area (fig. 3). The diorite is Late Jurassic (Stone and others, 2021).

Sample 16-LM-1342 is from a black, medium-grained, pure quartzite exposed along a pole-line road that extends northwest from Fort Irwin Road. This quartzite is underlain by thin-bedded calc-silicate hornfels. Zircons from this sample yielded 95 acceptable ages ranging from ~3,250 to 949 Ma (table 4) with a moderate peak at ~2,660 Ma, a major peak at ~1,818 Ma, and a group of three grains at ~1,093, 1,030, and 949 Ma (fig. 6*E*). The maximum depositional age of the sample is questionably interpreted as ~949 Ma on the basis of the youngest single grain (YSG; table 6); the youngest eight-grain cluster has a weighted mean age of ~1,702 Ma (YC1σ[2+]; fig. 7*Q*, table 6).

Igneous and Metamorphic Zircon Geochronology

As previously noted, six of the 23 samples analyzed for this report yielded zircons interpreted as metamorphic or igneous. These consist of a quartzite from which all the dated zircons are interpreted as metamorphic, and five fine- to medium-grained rocks that were initially thought to be of sedimentary origin but were later interpreted as igneous. This section presents the geochronological results for each of these six samples, beginning with the quartzite sample (17-LM-1349), followed by a group of three samples (15-LM-600, 17-LM-2032, and 18-LM-2939) interpreted as albitized igneous rocks of granitic to monzonitic composition, and finally by two samples (17-LM-1984 and 18-LM-2824) interpreted as fine-grained intrusive rocks of dioritic to monzonitic composition (tables 3, 4, 5; figs. 8, 9). The zircon data are filtered for age discordance (<15 percent positive or negative) but not for the other criteria applied to the detrital zircons.

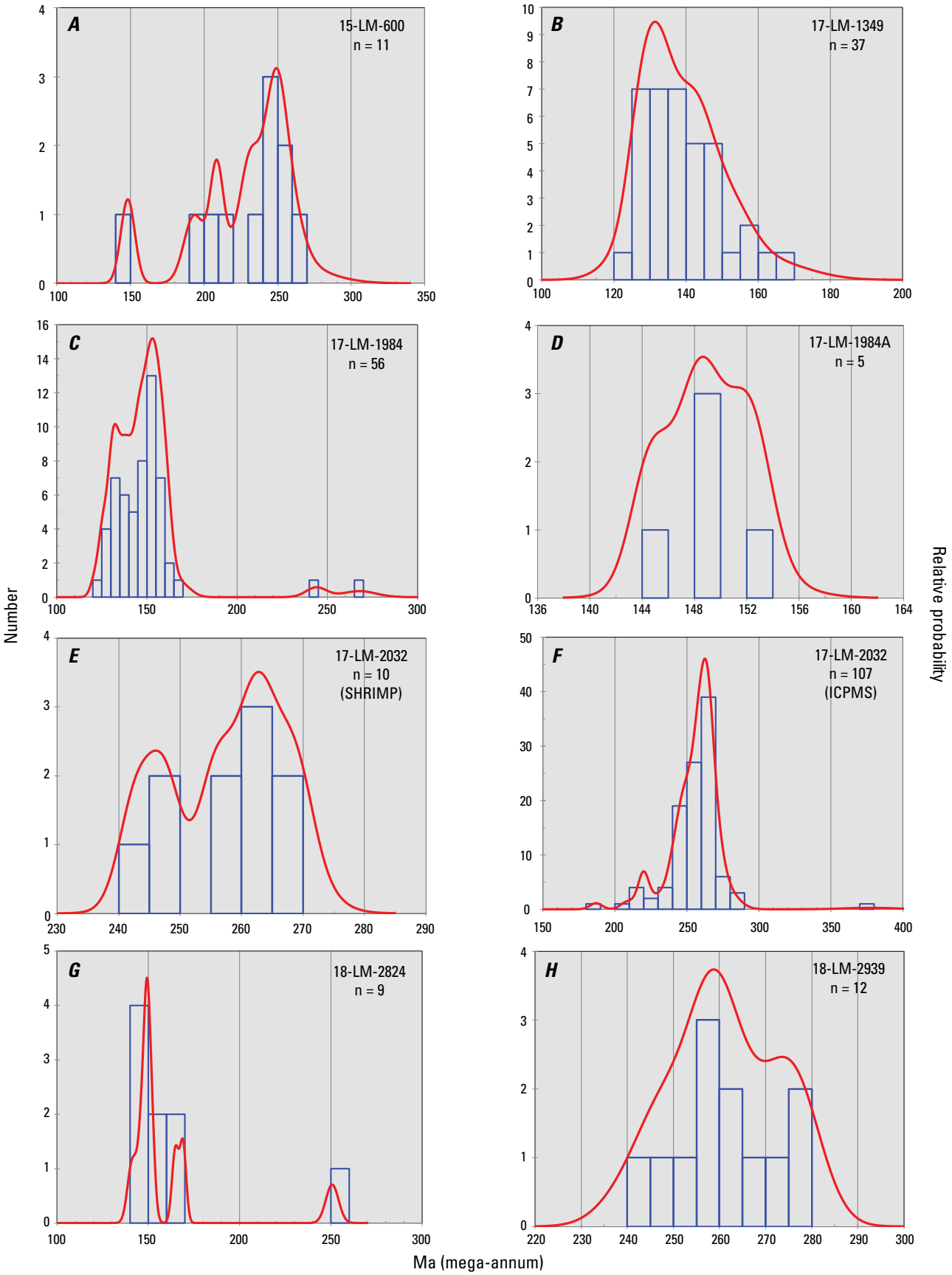

Figure 8. Probability density curves (red) and histograms (blue) of acceptable zircon ages from samples 15-LM-600 (*A*), 17-LM-1349 (*B*), 17-LM-1984 (*C*), 17-LM-1984A (*D*), 17-LM-2032 (*E*, *F*), 18-LM-2824 (*G*), and 18-LM-2939 (*H*). Zircon ages from sample 17-LM-1349 are interpreted as metamorphic; zircon ages from other samples are interpreted as magmatic. Left vertical axis shows number of grains analyzed from each sample; right vertical axis shows relative probability. Plots were created using Isoplot 4.15 (Ludwig, 2012) from data in tables 4 and 5 (available as supplemental files here: https://doi.org/10.3133/ofr20221115).

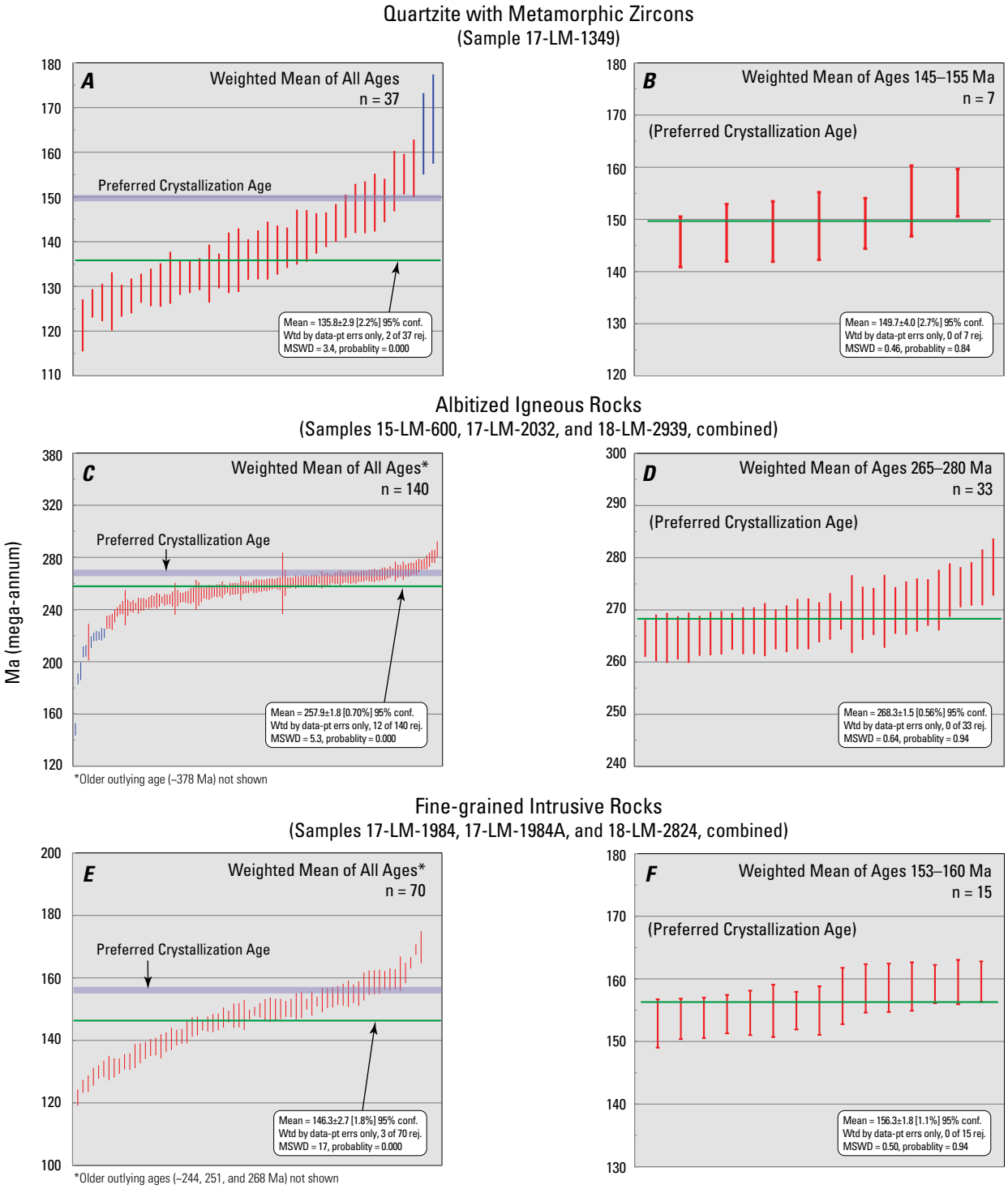

Figure 9. Weighted mean age plots of metamorphic zircons from quartzite sample 17-LM-1349 (*A*, *B*), magmatic zircons from albitized igneous rock samples 15-LM-600, 17-LM-2302, and 18-LM-2939, combined (*C*, *D*), and magmatic zircons from fine-grained intrusive rock samples 17-LM-1984, 17-LM-1984A, and 18-LM-2824, combined (*E*, *F*). *A*, *C*, and *E* show weighted means of all ages in each data set; *B*, *D*, and *F* show weighted means of selected age ranges in each data set, which are interpreted as the preferred crystallization ages. Plots were created using Isoplot 4.15 (Ludwig, 2012) from data in tables 4 and 5 (available as supplemental files here: https://doi.org/10.3133/ofr20221115). Vertical red bars represent individual zircon ages with 1σ error; horizontal green lines indicate weighted mean ages calculated by Isoplot. Horizontal blue lines were added manually to diagrams on left to show approximate preferred crystallization ages. Ma, millions of years; MSWD, Mean Squared Weighted Deviation.

Quartzite with Metamorphic Zircons

Sample 17-LM-1349

Sample 17-LM-1349 is from unit Pch_4 of the Carbide formation, which is near the structural top of that formation (table 1). This unit, which is intruded by Late Jurassic plutonic rocks (Stone and others, 2021), is composed primarily of massive calc-silicate rocks described as wollastonite-diopside hornfels by McCulloh (1960). The zircon sample was collected from an associated bed of light-gray, vitreous quartzite.

Zircons from sample 17-LM-1349 yielded 37 acceptable ages ranging from ~167 to 121 Ma (table 4) with an asymmetrical peak at ~131 Ma on a probability density plot (fig. 8*B*). This peak is defined by 32 zircons with ages less than ~150 Ma, coeval with or younger than the Late Jurassic plutonic rocks that intrude the upper part of the Carbide formation (Stone and others, 2021). In addition, all 37 zircons have unusually high U/Th ratios, most of them between 20 and 55. Together, the ages and U/Th ratios indicate that the zircons in sample 17-LM-1349 likely formed by post-depositional metamorphism and cannot be used to interpret the maximum depositional age.

The weighted mean of the 37 acceptable zircon ages from sample 17-LM-1349 is ~135 Ma (fig. 9*A*), but this cannot be assumed to represent the crystallization age because of the high mean squared weighted deviation (MSWD) of 3.4 and zero probability of fit, which reflect the large scatter of ages both above and below this value (Ludwig, 2012). In addition, metamorphism and zircon crystallization likely took place ~15 million years earlier, during intrusion of the Late Jurassic plutonic rocks. Therefore, we suggest that the crystallization age is represented by the older part of the data set (~155–145 Ma) and that the younger ages resulted from lead loss. Under this hypothesis, the ~150 Ma weighted mean of the seven ages in this range (with MSWD = 0.46 and probability of fit = 0.84; fig. 9*B*) is here interpreted as the approximate age of crystallization and metamorphism.

Albitized Igneous Rocks

Samples 15-LM-600, 17-LM-2032, and 18-LM-2939

Samples 15-LM-600, 17-LM-2032, and 18-LM-2939 are from a distinctive set of sheared, red-weathering rocks associated with unit Pcq_1 of the Carbide formation (McCulloh, 1960) near intrusive contacts with Permian to Triassic plutonic rocks (Stone and others, 2021; fig. 3). As seen in thin section, these rocks are largely composed of ~0.5 mm plagioclase grains that are separated by thin seams of red groundmass or matrix material; high sodium-potassium ratios determined by whole-rock chemical analyses (presented later) indicate that the plagioclase is albite. The rocks were initially thought to be an unusual type of albite-rich metasandstone on the basis of texture and geochemistry, and sample 17-LM-2032 was collected for detrital zircons. However, that sample yielded extremely abundant euhedral zircons that were mostly close in age to the adjacent Permian to Triassic plutonic rocks, casting doubt on the assumption that the zircons were detrital grains in a metasedimentary rock. Zircons from the lithologically similar samples 15-LM-600 and 18-LM-2939 were later analyzed to check for consistency with the results from sample 17-LM-2032. It was ultimately concluded that the sampled rocks likely originated as igneous bodies, probably intrusions, that were later sheared and albitized.

ICP-AES-MS analysis of zircons from sample 17-LM-2032 yielded 107 acceptable ages, 105 of which are ~286–208 Ma (table 4) with a major peak at ~263 Ma and a minor peak at ~220 Ma on a probability density diagram (fig. 8*F*). A supplementary SHRIMP analysis of sample 17-LM-2032 yielded 10 additional acceptable ages with a range of ~269–243 Ma (table 5) and peaks at ~263 and 246 Ma (fig. 8*E*). SHRIMP analysis of 12 zircons from sample 18-LM-2939 yielded 12 acceptable ages of ~278–242 Ma (table 5) with a peak at ~258 Ma (fig. 8*H*). Finally, SHRIMP analysis of 12 zircons from sample 15-LM-600 yielded 11 acceptable ages of ~260–148 Ma with a peak at ~250 Ma defined by the six oldest grains (~260–241 Ma; fig. 8*A*). All the zircon ages from samples 18-LM-2939 and 15-LM-600 are within the age range of the larger sample 17-LM-2032 except one very young (~148 Ma) age in sample 15-LM-600, consistent with the interpretation that all three samples represent a single geologic unit.

The weighted mean of all 140 acceptable ages from samples 15-LM-600, 17-LM-2032, and 18-LM-2939 combined is ~258 Ma, or late Permian (fig. 9*C*). However, as in the case of sample 17-LM-1349, the high MSWD (4.6) and zero probability of fit reflect the large scatter of the data and indicate that this cannot be assumed to be the age of crystallization. Instead, we suggest that the crystallization age is represented by the older part of the combined data set (~280–265 Ma) and that the younger ages are due to lead loss. The 33 ages within this range yield a middle Permian weighted mean age of ~268 Ma (with MSWD = 0.81 and probability of fit = 0.83; fig. 9*D*) that is here interpreted as the approximate crystallization age of the original igneous rock.

Fine-grained Intrusive Rocks

Samples 17-LM-1984 and 18-LM-2824

Samples 17-LM-1984 and 18-LM-2824 are from dark-gray, fine-grained rocks that appeared to be of metasedimentary character both in the field and when examined in thin section owing to their lack of an obvious igneous texture. Sample 18-LM-2824 is from an outcrop mapped as part of the Noble Well formation by McCulloh (1960), and sample 17-LM-1984 is from a lithologically similar outcrop that McCulloh (1960) did not map but was discovered by the authors and initially interpreted as metasedimentary (fig. 3). Both sample localities are surrounded and apparently intruded by coarse-grained plutonic rocks of Late Jurassic age (Stone and others, 2021). However, ICP-AES-MS analysis of zircons from sample 17-LM-1984 yielded ages about the same as and younger than

the surrounding plutonic rocks, raising doubt that these zircons could be detrital. To check on this unexpected result, a duplicate sample (17-LM-1984A) was collected from the same site, and a SHRIMP analysis of zircons from it yielded similar ages. Later SHRIMP analysis of zircons from sample 18-LM-2824 also yielded a similar result. It was ultimately concluded that these samples were fine-grained intrusive rocks and the zircons magmatic. Chemical analysis shows that sample 17-LM-1984A is of dioritic composition and sample 18-LM-2824 is of monzonitic composition (see "Geochemistry" section).

Subsequent detailed field examination of the area around the locality of sample 18-LM-2824 by the authors has shown that rocks like that sample grade laterally into very dark gray, fine- to medium-grained diorite with an obvious igneous texture, some outcrops of which were mapped as "hornfelsed diorite porphyry" by McCulloh (1960). Rocks like sample 18-LM-2824 also grade laterally into laminated calc-hornfels of undoubted metasedimentary origin. These relations indicate that sample 18-LM-2824 and, by inference, sample 17-LM-1984, may represent a hybrid lithology resulting from partial assimilation of metasedimentary country rocks by intrusive, fine-grained plutonic rocks.

ICP-AES-MS analysis of zircons from sample 17-LM-1984 yielded 56 acceptable ages with a range of ~268–122 Ma (table 4) and a Late Jurassic peak at ~152 Ma (fig. 8*C*). The two oldest ages (~268 and 244 Ma) could represent entrained detrital zircons; all the other ages are ~170 Ma and younger. SHRIMP analysis of sample 17-LM-1984A yielded five acceptable ages of ~152–145 Ma (table 5, fig. 8*D*), well within the range of sample 17-LM-1984. SHRIMP analysis of sample 18-LM-2824 yielded nine acceptable ages with a range of ~251–141 Ma (table 5) and a peak at ~149 Ma (fig. 8*G*), again within the range of sample 17-LM-1984 and with one older age (~251 Ma) that could represent an entrained detrital zircon. These results support the interpretation that samples 17-LM-1984 and 18-LM-2824 represent the same geologic unit.

The weighted mean age of the 70 acceptable ages from samples 17-LM-1984, 17-LM-1984A, and 18-LM-2824 combined is ~146 Ma (fig. 9*E*), but the high MSWD (17) and zero probability of fit show that this cannot be assumed to represent the age of crystallization. Instead, we suggest that the crystallization age is likely at the older end of the data set (between ~160 and 150 Ma) and that all younger ages reflect various degrees of lead loss. Several slightly different solutions are possible under this hypothesis, but the preferred crystallization age is here interpreted to be ~156 Ma, the weighted mean of 15 ages between ~160 and 153 Ma with MSWD = 0.5 and probability of fit = 0.94 (fig. 9*F)*.

A possible alternative interpretation is that the sampled rocks are metasedimentary rather than intrusive and that the zircons are not Jurassic magmatic crystals but instead are older detrital grains that underwent extreme, post-depositional lead loss related to Late Jurassic plutonism. This interpretation would be similar to that reported by Clemens-Knott and Gevedon (2022) for Jurassic zircons in the northern El Paso terrane in the southeastern Sierra Nevada.

Geochemistry

Chemical analyses were obtained for the three samples interpreted as albitized Permian to Triassic igneous rocks (15-LM-600, 17-LM-2032, and 18-LM-2939) and the two samples interpreted as Late Jurassic fine-grained plutonic rocks (17-LM-1984A and 18-LM-2824). The data are listed in table 7, and a total alkali-silica (TAS) diagram of the normalized WDXRF data is presented in figure 10.

Samples 17-LM-2032 and 18-LM-2939 are chemically similar, plotting within the granite and quartz monzonite fields of the TAS diagram, respectively. In addition, both samples are enriched in sodium and depleted in potassium, with Na_2O:K_2O ratios of ~12 and 80, respectively. These ratios indicate that these rocks have undergone intense sodium metasomatism, presumably by albitization of the original feldspars. Sample 15-LM-600 is chemically different, plotting as monzonite (fig. 10), but has a similarly high Na_2O:K_2O ratio of ~12. The chemical data are consistent with the interpretation of these rocks as albitized intrusions.

Samples 17-LM-1984A and 18-LM-2824 are chemically similar, with ~57 and 58 weight percent SiO_2, respectively. Sample 17-LM-1984A is the more alkalic of the two and falls marginally into the monzonite field of the TAS diagram, whereas sample 18-LM-2824 plots as diorite (fig. 10). Both compositions are in the range determined for coarser grained, Late Jurassic plutonic rocks in the Lane Mountain area by Stone and others (2021) and are thus compatible with the interpretation that these rocks are fine-grained variants of the same plutonic suite.

Table 7. ICP-AES-MS and WDXRF geochemical analyses of samples included in this report.

[Inductively coupled plasma atomic emission spectroscopy-mass spectrometry (ICP-AES-MS) data: Numerical values are in weight percent (%) or parts per million (ppm), as indicated. Si, silicon; Ti, titanium, Al, aluminum; Mg, magnesium; Fe, iron; Ca, calcium; K, potassium; P, phosphorus; S, sulfur; Li, lithium; Be, beryllium; B, boron; Sc, scandium; V, vanadium; Cr, chromium; Mn, manganese; Co, cobalt; Ni, nickel; Cu, copper; Zn, zinc; Ga, gallium; Ge, germanium; As, arsenic; Se, selenium; Rb, rubidium; Sr, strontium; Y, yttrium; Zr, zirconium; Nb, niobium; Mo, molybdenum; Ag, silver; Cd, cadmium; In, indium; Sn, tin; Sb, antimony; Te, tellurium; Cs, cesium; Ba, barium; Hf, hafnium; Ta, tantalum; W, tungsten; Tl, thallium; Pb, lead; Bi, bismuth; Th, thorium; U, uranium; La, lanthanum; Ce, cerium; Pr, praseodymium; Nd, neodymium; Sm, samarium; Eu, europium; Gd, gadolinium; Tb, terbium; Dy, dysprosium; Ho, holmium; Er, erbium; Tm, thulium; Yb, ytterbium; Lu, lutetium. Wavelength dispersive X-ray fluorescence (WDXRF) data: Numerical values are in weight percent. LOI, loss on ignition. Data can be found in data release, Stone and others (2023), https://doi.org/10.5066/P9G6YNEF.]

Elements	Samples				
	15-LM-600	17-LM-1984A	17-LM-2032	18-LM-2824	18-LM-2939
ICP-AES-MS (percent)					
Si	28.7	28.2	33.4	28.6	32.7
Ti	0.61	0.59	0.27	0.48	0.41
Al	9.62	9.3	8.96	8.97	9.35
Mg	1.98	0.95	0.09	2.5	0.03
Fe	3.11	5.47	1.83	5.03	1.75
Ca	4.08	7.25	0.54	7.71	0.68
K	0.47	3.65	0.61	0.98	0.12
P	0.06	0.14	0.06	0.13	0.05
S	0.2	<0.1	0.4	<0.1	0.1
ICP-AES-MS (parts per million)					
Li	<10	20	<10	<10	<10
Be	<5	<5	<5	<5	<5
B	<10	23	<10	<10	<10
Sc	21	17	6	21	<5
V	202	176	62	219	58
Cr	<10	12	<10	27	<10
Mn	394	1,160	<10	1,360	<10
Co	2.9	16.5	0.5	18.9	1.6
Ni	<5	9	<5	14	<5
Cu	24	<5	18	17	<5
Zn	15	48	<5	65	<5
Ga	21.9	22.2	14.3	19.5	19
Ge	2	3	1	2	1
As	<5	10	<5	<5	<5
Se	<5	10	<5	<5	<5
Rb	11.2	131	9.2	17.4	1.3
Sr	510	307	260	259	139
Y	16.9	25.6	7.9	21.4	6
Zr	122	139	98.1	163	122
Nb	7.2	9.2	6	8.7	8.5
Mo	<2	2	4	<2	4
Ag	<1	<1	<1	<1	<1
Cd	<0.2	<0.2	<0.2	<0.2	<0.2
In	<0.2	<0.2	<0.2	<0.2	<0.2
Sn	2	1	<1	1	1
Sb	0.2	4.2	<0.1	3.3	<0.1
Te	<0.5	<0.5	<0.5	<0.5	<0.5
Cs	0.6	8	0.3	0.6	<0.1
Ba	252	1,880	328	402	54.4
Hf	4	4	3	5	4
Ta	1	0.8	0.6	<0.5	<0.5
W	<1	3	2	<1	3
Tl	<0.5	1.5	1	1.6	1.6

Table 7. ICP-AES-MS and WDXRF geochemical analyses of samples included in this report.—Continued

Elements	Samples				
	15-LM-600	17-LM-1984A	17-LM-2032	18-LM-2824	18-LM-2939
Pb	<5	8	<5	<5	<5
Bi	0.2	<0.1	0.2	<0.1	0.2
Th	1.1	5.1	2.6	5.8	4.1
U	0.51	1.44	0.93	2.16	1.55
La	8.7	24.5	9.7	22.9	3.3
Ce	19.3	54.4	17.4	48.2	7
Pr	2.7	7.11	1.94	6.05	0.91
Nd	11.2	28.9	6.4	24.5	3.4
Sm	2.8	6.1	1.2	5.1	0.7
Eu	0.84	2.04	0.37	1.33	0.2
Gd	2.9	5.67	1.07	4.55	0.74
Tb	0.51	0.84	0.16	0.69	0.12
Dy	3.41	4.76	1.09	3.95	0.88
Ho	0.7	0.99	0.25	0.8	0.21
Er	2.1	2.83	0.89	2.28	0.65
Tm	0.33	0.43	0.14	0.35	0.11
Yb	2.2	2.8	1	2.3	0.7
Lu	0.32	0.43	0.17	0.37	0.12
WDXRF (weight percent)					
SiO_2	60	56.6	68.9	58	68
TiO_2	1.01	0.97	0.43	0.79	0.66
Al_2O_3	17.7	16.8	16.4	16.2	17.2
MgO	3.19	1.51	0.13	4	0.04
Fe_2O_3	4.3	7.51	2.47	6.89	2.39
MnO	0.05	0.16	<0.01	0.18	<0.01
CaO	5.58	9.62	0.72	10.1	0.9
K_2O	0.52	4.14	0.68	1.1	0.12
Na_2O	6.24	1.92	8	2.24	9.55
P_2O_5	0.12	0.3	0.13	0.29	0.12
Cr_2O_3	<0.01	<0.01	<0.01	<0.01	<0.01
V_2O_5	0.04	0.03	0.01	0.04	0.01
SrO	0.06	0.03	0.03	0.02	<0.01
BaO	0.02	0.21	0.03	0.04	<0.01
LOI	1.85	0.49	2.21	0.58	1.01
WDXRF (normalized weight percent; volatile free)					
SiO_2	60.7	56.7	70.4	58.1	68.7
TiO_2	1.02	0.97	0.44	0.79	0.67
Al_2O_3	17.9	16.8	16.7	16.2	17.4
MgO	3.23	1.51	0.13	4	0.04
Fe_2O_3	4.35	7.53	2.52	6.90	2.41
MnO	0.05	0.16	<0.01	0.18	<0.01
CaO	5.65	9.64	0.74	10.1	0.91
K_2O	0.53	4.15	0.69	1.1	0.12
Na_2O	6.31	1.92	8.17	2.24	9.65
P_2O_5	0.12	0.3	0.13	0.29	0.12
Cr_2O_3	<0.01	<0.01	<0.01	<0.01	<0.01
V_2O_5	0.04	0.03	0.01	0.04	0.01
SrO	0.06	0.03	0.03	0.02	<0.01
BaO	0.02	0.21	0.03	0.04	<0.01
K_2O+Na_2O	6.84	6.07	8.86	3.35	9.77

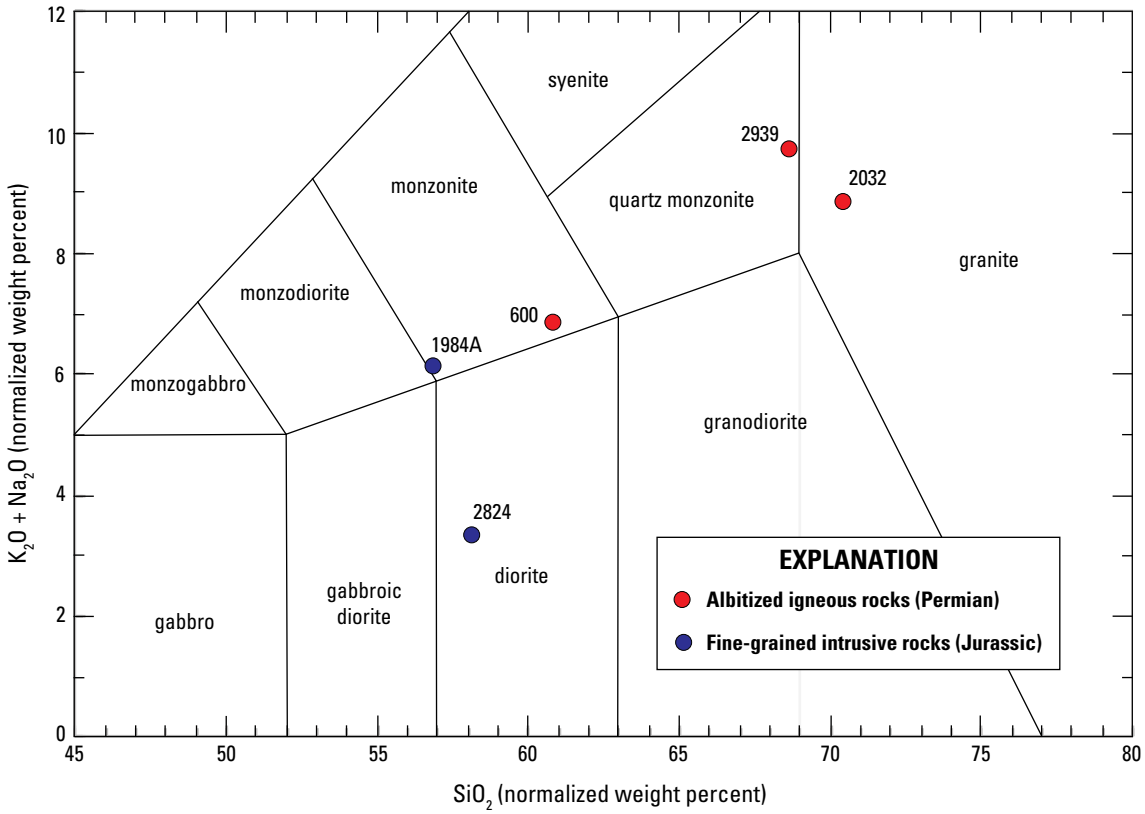

Figure 10. Modified total alkali-silica (TAS) diagram (Middlemost, 1994) showing geochemical classification of albitized igneous rock samples of Permian age (15-LM-600, 17-LM-2032, and 18-LM-2939) and fine-grained intrusive rock samples of Jurassic age (17-LM-1984A and 18-LM-2824).

Discussion

Detrital Zircon Overview

The 17 detrital zircon samples analyzed in this study yielded a total of 885 acceptable ages that range from ~3,254 to 173 Ma. A composite plot of these ages (fig. 11) shows a notable concentration between ~2,800 and 2,400 Ma, a larger concentration between ~2,100 and 1,600 Ma with a well-defined peak at ~1,835 Ma, and a major concentration between ~300 and 200 Ma. A plot of the detrital zircon ages <400 Ma provides details of the youngest concentration, including a major peak at ~268 Ma, a lesser peak at ~213 Ma, and a minor peak at ~197 Ma. Ages between ~1,600 and 300 Ma are broadly distributed with no significant peaks and relatively few ages between ~900 and 600 Ma.

The composite age distribution indicates two major source areas: a continental source of Archean and Proterozoic zircons, presumably ancestral North America, and a younger source of late Paleozoic to early Mesozoic zircons, presumably the magmatic arc interpreted to have developed along the western margin of ancestral North America during Permian to Triassic time (Barth and others, 1997). In the area of figure 1 and to the south, this arc is represented by plutonic rocks that range in age from ~275 to 210 Ma, encompassing all but the youngest detrital zircon ages at Lane Mountain (Barth and Wooden, 2006; Cecil and others, 2019). Among others, these plutons include those that intrude the western margin of the El Paso terrane in both the Lane Mountain area (Stone and others, 2021) and the El Paso Mountains (Carr and others, 1997; Cecil and others, 2019).

The major detrital zircon age peak at ~268 Ma is somewhat puzzling because only a few dated plutons in the area of figure 1 and to the south are >260 Ma, and most are ~250 Ma or younger. For example, Permian to Triassic plutonic rocks dated by Stone and others (2021) in the Lane Mountain area have an average age of ~248 Ma. Thus, the age distribution could mean that (1) arc rocks >260 Ma were once abundant in the general vicinity of the Lane Mountain area but are not widely exposed, (2) the zircons were transported as sediment from more distant, older parts of the arc, or (3) large-magnitude, post-depositional faulting has displaced the El Paso terrane, including the Lane Mountain area, from the source of these relatively old detrital zircons.

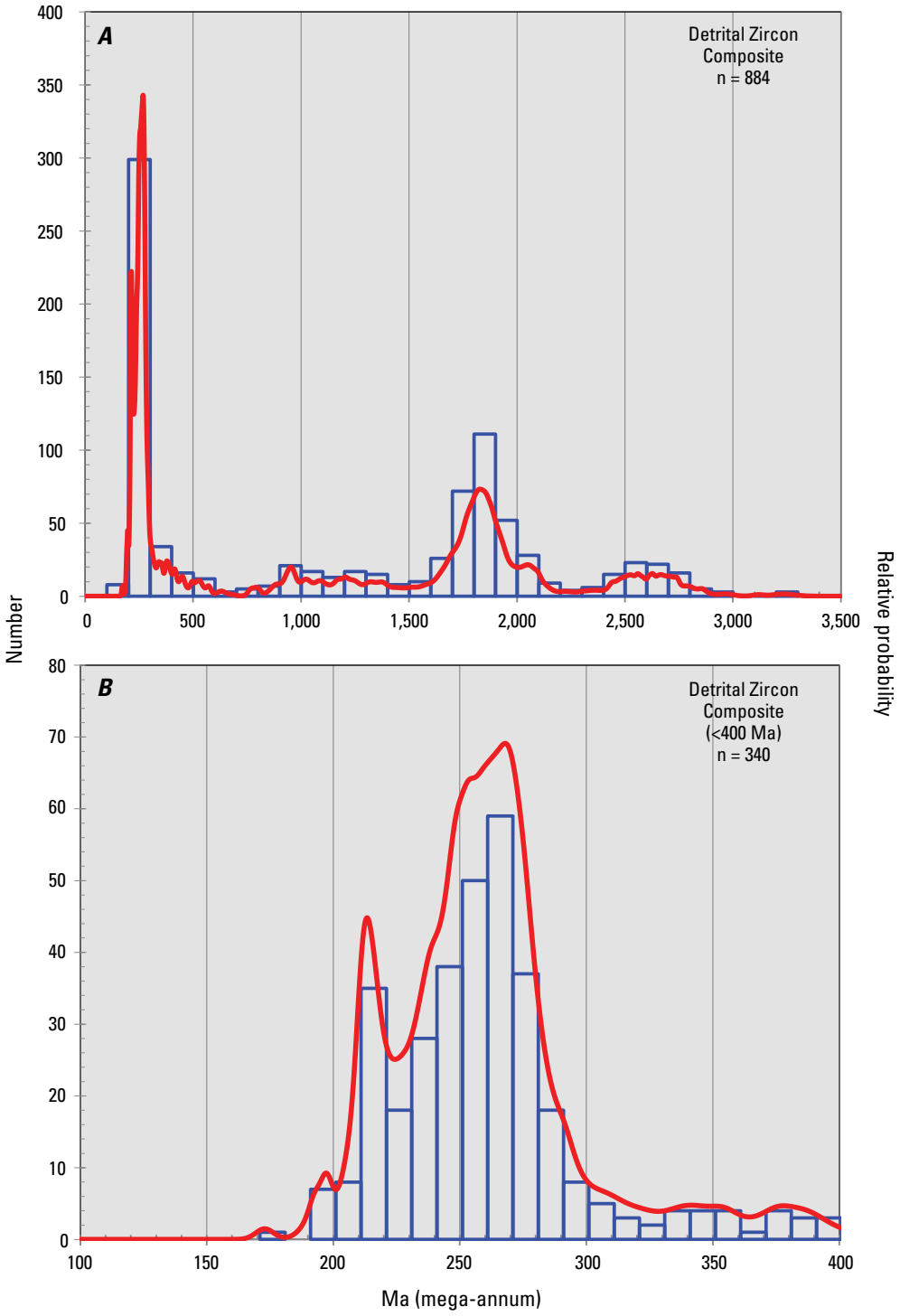

Figure 11. Composite probability density curves (red) and histograms (blue) of zircon ages from all 17 detrital zircon samples analyzed for this report. *A*, all acceptable ages as defined in text; *B*, acceptable ages <400 Ma. Plots were created using Isoplot 4.15 (Ludwig, 2012) from data in tables 4 and 5 (available as supplemental files here: https://doi.org/10.3133/ofr20221115). Left vertical axis shows number of grains; right vertical axis shows relative probability.

Detrital Zircon Stratigraphy

Carbide Formation

Detrital zircon data from the Carbide formation indicate that most of the units mapped by McCulloh (1960) within this thick structural sequence (table 1) are generally upright and in stratigraphic order from west to east. The three structurally lowest units (Pca, Pcq_1, and Pcmcg) are provisionally interpreted as middle Paleozoic on the basis of sparse detrital zircons from samples 15-LM-921, 16-LM-1215, and 18-LM-2738. This age interpretation, although not definitive, is consistent with the fact that unit Pca and the lower part of unit Pcq_1 are intruded by Permian to Triassic plutonic rocks (Stone and others, 2021). The Pennsylvanian or Permian age indicated by the reported presence of fusulinids in unit Pcmcg (Rich, 1961) has not been confirmed by the zircon data presently available.

No zircon data are available for the overlying unit Pcmc, but the sequence of units above that (Pch_1–Pcq_2) is here interpreted as Triassic (probably no older than ~230 Ma) on the basis of detrital zircons from samples 14-LM-60, 15-LM-1012, 15-LM-1085, and 15-LM-1173. Therefore, we suggest that the lower ~7,650 m of the Carbide formation is a deformed stratigraphic sequence rather than a structural stack of unrelated thrust sheets. Notably, the strata interpreted as Triassic in age are evidently younger than the Permian to Triassic (~248 Ma) plutonic rocks that intrude the structurally lower part of the Carbide formation.

By contrast, the structurally higher quartzite samples 15-LM-1050 and 15-LM-1135 yielded only Precambrian zircons and are likely older than the underlying rocks. The quartzite of sample 15-LM-1135 is in unit Pcu_1 of McCulloh (1960) and that of sample 15-LM-1050 is in the upper part of unit Pcq_2 (table 1). However, the quartzite of sample 15-LM-1050 is probably unrelated to the underlying part of unit Pcq_2. We suggest that the quartzite of sample 15-LM-1050 is related to that of sample 15-LM-1135. The black quartzite sample 16-LM-1342 from an outcrop not mapped by McCulloh (1960) also yielded only Precambrian zircons and could be stratigraphically related to lithologically similar, black quartzites in the general vicinity of sample 15-LM-1135.

These three quartzite samples all have similar Precambrian zircon age profiles that feature a prominent peak between ~1,820 and 1,860 Ma. These profiles resemble that of western North American quartz sandstones of early Paleozoic age, including the Ordovician Eureka Quartzite (Workman, 2012; Gehrels and Pecha, 2014), which indicates a possible chronostratigraphic correlation. Unpublished mapping by the authors indicates the possibility that the metasedimentary units containing these quartzites, together with the Late Jurassic plutonic rocks that intrude them, were thrust above the younger, underlying rocks of the Carbide formation in Cretaceous time (Paul Stone, U.S. Geological Survey, 2020).

The other two samples of detrital zircons from the Carbide formation (15-LM-883 and 15-LM-888), from unit Pcq_1 below the Williams Well formation in the northern part of the report area (fig. 3), are problematic. Both samples are dominated by Precambrian zircons that yield similar, well-defined Archean and Paleoproterozoic age peaks (fig. 4), and sample 15-LM-883 additionally contains a few younger grains interpreted to indicate a maximum depositional age of ~250 Ma. These age profiles differ from those of the other samples (15-LM-921 and 18-LM-2738) from unit Pcq_1, and the coarse-grained to conglomeratic textures of quartzite samples 15-LM-883 and 15-LM-888 are also distinct. These differences indicate that samples 15-LM-883 and 15-LM-888 may represent a geologic unit separate from other rocks mapped as unit Pcq_1 by McCulloh (1960).

Williams Well and Starbright Formations

A single detrital zircon sample (15-LM-894) from the Williams Well formation is interpreted to indicate a late Paleozoic (early Permian) maximum depositional age, although most of its zircons are Precambrian. No detrital zircon data are available for the carbonate rocks of the Starbright formation, which McCulloh (1960) mapped as faulted above the Williams Well formation.

Noble Well Formation

Detrital zircon data from the Noble Well formation show substantial differences between the lithologically distinct, southern and northern units recognized herein. In particular, the dominant ~215–210 Ma age peak of southern samples 14-LM-128 and 15-LM-930 is distinct from the ~260–235 Ma age peaks of northern samples 15-LM-909 and 15-LM-910, possibly signifying derivation from different parts of the Permian to Triassic magmatic arc. However, data from both units indicate an Early Jurassic (~194–192 Ma) maximum depositional age, which is compatible with unpublished fossil evidence compiled decades ago by T.H. McCulloh (U.S. Geological Survey, written commun., 1960; see appendix 1) and confirms that the formation is Jurassic.

Previously, the age of the Noble Well formation was interpreted as Early Triassic (Walker, 1987, 1988), and plutonic rocks dated as ~240 Ma by Miller and others (1995) were interpreted as continuous with those intrusive into that formation. Data presented in this report and by Stone and others (2021) demonstrate that the Noble Well formation is more than 40 million years younger than the ~240 Ma plutonic rocks of Miller and others (1995) and that the plutonic rocks intrusive into the Noble Well formation are of Late Jurassic age.

The geologic map of McCulloh (1960) portrays the Noble Well formation as allochthonous with respect to the underlying rocks, which include the Starbright formation, the Williams Well formation, and the lower part of the Carbide formation (fig. 3). Mapping by the authors supports this interpretation and further indicates that the Noble Well formation and the Late Jurassic plutonic rocks that intrude it may be part of the same thrust sheet as quartzite samples 15-LM-1050, 15-LM-1135, and 16-LM-1342 of the Carbide formation. Additional mapping is needed to test this interpretation and delineate the full extent of the allochthonous rocks.

Regional Detrital Zircon Comparisons

The age profiles of Precambrian detrital zircons in quartzite samples 15-LM-1050, 15-LM-1135, and 16-LM-1342 from the Lane Mountain area resemble that reported by Attia and others (2018) from deep-marine strata of inferred Ordovician age in the southeastern Sierra Nevada, which represent the northwesternmost known part of the El Paso terrane (fig. 1). The Sierra Nevadan samples show a major age peak at ~1,850 Ma and minor peaks at ~2,700 and 2,500 Ma, indicating a possible chronostratigraphic correlation with the Lane Mountain quartzites. As pointed out by Attia and others (2018), a similar zircon age distribution also characterizes Ordovician strata in the Roberts Mountains allochthon of Nevada. The most likely source of these Precambrian zircons is commonly interpreted as the Peace River Arch of northwestern British Columbia, Canada (Gehrels and Pecha, 2014), although other possible sources have also been suggested (Workman, 2012).

The detrital zircon age distribution that characterizes samples 15-LM-1085 and 15-LM-1173 from Carbide formation unit Pcq_2 at Lane Mountain resembles that reported by McDonald (2016) from two samples in the upper part of the sedimentary rocks of Holland Camp (Carr and others, 1997) in the El Paso Mountains (fig. 1). Like the Lane Mountain samples, each of those samples has a dominant Permian peak age (~267 and ~264 Ma) that indicates a source area in the Permian to Triassic arc. However, unlike the Lane Mountain samples, which contain numerous Triassic zircons, those from the El Paso Mountains yielded only a single, anomalous zircon <250 Ma and are therefore interpreted as older. In addition, the rocks sampled by McDonald (2016) are volcaniclastic and yielded few Precambrian zircons, which is interpreted to indicate closer proximity to the arc and a longer distance from the continental margin than the quartzitic rocks at Lane Mountain. Additional information on the detrital zircons from the El Paso Mountains is provided by McDonald and others (2016a, b, 2018).

The Early Jurassic (~192–194 Ma) maximum depositional age defined by detrital zircons from the Noble Well formation in the Lane Mountain area closely matches that determined by Stone and others (2013) for the Fairview Valley Formation of Bowen (1954) in the Black Mountain-Quartzite Mountain area ~30 km southwest of Barstow (fig. 1). This similarity supports the correlation first conceived (but never published) by T.H. McCulloh between the Noble Well formation and the Fairview Valley Formation based on comparable lithology and generally similar paleontological age constraints (T.H. McCulloh, U.S. Geological Survey, written commun., 1960; see appendix 1). Walker (1987) also noted this possible correlation. Our own work, including Stone (2006), Stone and others (2013), and Brown (2017), confirms that both units contain very similar lithofacies of hornfels, metasandstone, and metaconglomerate, indicating that the two units are probably equivalent. On the basis of this interpretation, the younger age limit of the Noble Well formation is inferred to be ~181 Ma (late Early Jurassic), the age of the tuff of Black Mountain, which overlies the Fairview Valley Formation (Fohey-Breting and others, 2010; Stone and others, 2013).

Implications for the El Paso terrane

The depositional history of the El Paso terrane is generally considered to have ended in the Permian, when the stratigraphic sequence was deformed and then intruded by plutons of the Permian to Triassic arc (Miller and Sutter, 1982; Carr and others, 1997). The results of this study, however, show that both deposition and deformation in the Lane Mountain sector of the El Paso terrane continued into the Triassic, after the intrusion of ~248-Ma plutons of the arc, and even into the Jurassic if the Noble Well formation is considered part of the terrane. Although beyond the scope of the present report, this expanded geologic history will require revisions of existing tectonic models that involve the El Paso terrane and its relation to the evolution of the continental margin.

Summary

This study was undertaken to constrain the ages of the metasedimentary rock units mapped by McCulloh (1952, 1960) in the Lane Mountain area using U-Pb detrital zircon geochronology. Metasedimentary and metavolcanic rocks in this area are considered part of the El Paso terrane, which is commonly interpreted as substantially displaced, although its detailed history is poorly understood.

Geochronologic analysis of 23 samples shows that 17 of these contain zircons of detrital origin. These samples represent the informally named Carbide, Williams Well, and Noble Well formations of McCulloh (1960). The other six samples were originally thought to be metasedimentary but were later reinterpreted as metamorphic or igneous.

The detrital zircon data indicate that the units that make up the lower ~7,650 meters (m) of the Carbide formation appear to comprise a deformed stratigraphic sequence with maximum depositional ages ranging from middle or late Paleozoic to Triassic. By contrast, quartzites in the structurally highest units of the Carbide formation yielded only Precambrian zircons that indicate a possible Ordovician depositional age based on comparison with detrital zircon age profiles of known Ordovician sandstones, including the Eureka Quartzite. The metasedimentary units containing these quartzites, together with the Late Jurassic plutonic rocks that intrude them, are interpreted to have been thrust above the underlying units in Cretaceous time.

Detrital zircons from the Williams Well formation, which McCulloh (1960) mapped as faulted above the underlying rocks of the Carbide formation, suggest a late Paleozoic maximum depositional age. Rocks of the structurally overlying Starbright formation of McCulloh (1960) were not sampled for detrital zircons.

Detrital zircons from the Noble Well formation indicate an Early Jurassic maximum depositional age consistent with the sparse paleontological data that are available. The Noble Well formation lies structurally above the lower part of the

Carbide formation and may be part of the same thrust sheet as the possible Ordovician quartzites in the upper part of the Carbide formation. The Noble Well formation is interpreted as equivalent to the lithologically similar, Early Jurassic Fairview Valley Formation exposed ~60 km to the south.

As interpreted above, the detrital zircon ages reported here indicate that the depositional, magmatic, and deformational history of the El Paso terrane was longer and more complex than previously thought and will require revisions of existing tectonic models involving this terrane. Further study, however, is needed to ensure that the reported ages were not reset by extreme post-depositional lead loss.

Acknowledgments

This work was funded by the U.S. Geological Survey (USGS) National Cooperative Geologic Mapping Program and was conducted under the project leadership of David Miller and Andrew Cyr. Juliet Ryan-Davis and Nicole Thomas provided invaluable guidance and support as managers of the USGS mineral separation laboratory in Menlo Park. Geochronologic sample preparation and zircon separations were performed by Randy Woods, who also assisted with the SHRIMP-RG analyses. Marsha Lidzbarski helped with preparation of the zircon mounts. Brad Ito and Eric Angel provided electronics support of the SHRIMP-RG. The authors also thank Diane Clemens-Knott (California State University, Fullerton) for enlightening discussions about extreme lead loss in detrital zircons and for testing its possible effects on the Lane Mountain detrital zircon dataset.

References Cited

Attia, S., Paterson, S.R., Cao, W., Chapman, A.D., Saleeby, J., Dunne, G., Stevens, C.H., and Memeti, V., 2018, Late Paleozoic tectonic assembly of the Sierra Nevada prebatholithic framework and western Laurentian provenance links based on synthesized detrital zircon geochronology, *in* Ingersoll, R.V., Lawton, T.F., and Graham, S.A., eds., Tectonics, sedimentary basins, and provenance; a celebration of William R. Dickinson's career: Geological Society of America Special Paper 540, p. 267–295, https://doi.org/10.1130/2018.2540(12).

Barth, A.P., Tosdal, R.M., Wooden, J.L., and Howard, K.A., 1997, Triassic plutonism in southern California—southward younging of arc initiation along a truncated continental margin: Tectonics, v. 16, no. 2, p. 290–304.

Barth, A.P., and Wooden, J.L., 2006, Timing of magmatism following initial convergence at a passive margin, southwestern U.S. Cordillera, and ages of lower crustal magma sources: Journal of Geology, v. 114, p. 231–245.

Bowen, O.E., Jr., 1954, Geology and mineral deposits of Barstow quadrangle, San Bernardino County, California: California Division of Mines Bulletin 165, p. 5–185, scale 1:125,000.

Brown, H.J., 2016a, Detailed geologic map of the northern Calico Mountains and the Lane Mountain area, central Mojave Desert, California; part 1, the need for new mapping [abs.]: Geological Society of America Abstracts with Programs, v. 48, no. 4, https://gsa.confex.com/gsa/2016CD/webprogram/Paper271692.html.

Brown, H.J., 2016b, Detailed geologic map of the northern Calico Mountains and the Lane Mountain area, central Mojave Desert, California; part 2, stratigraphy and structure of Paleozoic, Mesozoic, and Cenozoic rocks [abs.]: Geological Society of America Abstracts with Programs, v. 48, no. 4, https://gsa.confex.com/gsa/2016CD/webprogram/Paper271693.html.

Brown, H.J., 2017, Geology of the Cemex Inc. limestone quarries, Sidewinder Mountain–Black Mountain area, San Bernardino County, California, *in* Kraatz, B., Lackey, J.S., and Fryxell, J.E., eds., Field excursions in southern California; field guides to the 2016 GSA Cordilleran Section meeting: Geological Society of America Field Guide 45, p. 229–251, https://doi.org/10.1130/FLD045.

Brown, H.J., 2020, Pre-Miocene rocks and structures in the Lane Mountain-Calico Mountains area, central Mojave Desert area, California [abs.]: Geological Society of America Abstracts with Programs, v. 52, no. 4, https://gsa.confex.com/gsa/2020CD/meetingapp.cgi/Paper/346430.

Brown, H.J., Stone, P., Rosario, J., and Fitzpatrick, J., 2016, Detailed geologic map of the northern Calico Mountains and the Lane Mountain area, central Mojave Desert, California; part 3, preliminary digital geologic map [abs.]: Geological Society of America Abstracts with Programs, v. 48, no. 4, https://gsa.confex.com/gsa/2016CD/webprogram/Paper271694.html.

Brown, H.J., Stone, P., Cecil, M.R., and Fitzpatrick, J., 2018, New insights into the geology of the Lane Mountain and north Calico Mountains area, central Mojave Desert, California [abs.]: Geological Society of America Abstracts with Programs, v. 50, no. 5, https://gsa.confex.com/gsa/2018RM/meetingapp.cgi/Paper/311369.

Burchfiel, B.C., and Davis, G.A., 1981, Mojave Desert and environs, chap. 9 *of* Ernst, W.G., ed., The geotectonic development of California, Rubey Volume 1: Englewood Cliffs, N.J., Prentice-Hall, p. 217–252.

Burke, D.B., Hillhouse, J.W., McKee, E.H., Miller, S.T., and Morton, J.L., 1982, Cenozoic rocks in the Barstow area of southern California—Stratigraphic relations, radiometric ages, and paleomagnetism: U.S. Geological Survey Bulletin 1529-E, p. E1–E16.

Carr, M.D., Christiansen, R.L., Poole, F.G., and Goodge, J.W., 1997, Bedrock geologic map of the El Paso Mountains in the Garlock and El Paso Peaks 7½' quadrangles, Kern County, California: U.S. Geological Survey Miscellaneous Investigations Series Map I-2389, scale 1:24,000, 9 p.

Cecil, M.R., Ferrer, M.A., Riggs, N.R., Marsaglia, K., Kylander-Clark, A., Ducea, M.N., and Stone, P., 2019, Early arc development recorded in Permian–Triassic plutons of the northern Mojave Desert region, California, USA: Geological Society of America Bulletin, v. 131, no. 5/6, p. 749–765, https://doi.org/10.1130/B31963.1.

Clemens-Knott, D., and Gevedon, M., 2022, Using discordant zircon to re-evaluate the northern El Paso terrane; late Paleozoic tectonic evolution of southwestern Laurentia, extension of the Permian arc, and a Middle Jurassic hydrothermal event within the southeastern Sierra Nevada arc [abs.]: Geological Society of America Abstracts with Programs, v. 54, no. 2, https://gsa.confex.com/gsa/2022CD/meetingapp.cgi/Paper/373734.

Dibblee, T.W., Jr., 2008, Geologic map of the Opal Mountain and Lane Mountain 15-minute quadrangles, San Bernardino County, California: Santa Barbara, Calif., Dibblee Geology Center Map DF-403, scale 1:62,500.

Dickinson, W.R., and Gehrels, G.E., 2009, Use of U-Pb ages of detrital zircons to infer maximum depositional ages of strata; a test against a Colorado Plateau Mesozoic database: Earth and Planetary Science Letters, v. 288, p. 115–125, https://doi.org/10.1016/j.epsl.2009.09.013.

Fohey-Breting, N.K., Barth, A.P., Wooden, J.L., Mazdab, F.K., Carter, C.A., and Schermer, E.R., 2010, Relationship of voluminous ignimbrites to continental arc plutons; petrology of Jurassic ignimbrites and contemporaneous plutons in southern California: Journal of Volcanology and Geothermal Research, v. 189, p. 1–11, https://doi.org/10.1016/j.jvolgeores.2009.07.010.

Gehrels, G., and Pecha, M., 2014, Detrital U-Pb zircon geochronology and Hf isotope geochemistry of Paleozoic and Triassic passive margin strata of western North America: Geosphere, v. 10, no. 1, p. 49–65, https://doi.org/10.1130/GES00889.1.

Gradstein, F.M., Ogg, J.G., Schmitz, M.D., and Ogg, G.M., eds., 2020, Geologic time scale 2020: Cambridge, Mass., Elsevier, 1,357 p. (2 volumes).

Horie, K., Hidaka, H., and Gauthier-Lafaye, F., 2006, Elemental distribution in zircon; alteration and radiation-damage effects: Physics and chemistry of the Earth, v. 31, p. 587–592.

Jennings, C.W., Strand, R.G., and Rogers, T.H., 1977, Geologic map of California: California Division of Mines and Geology, scale 1:750,000.

Kistler, R.W., 1990, Two different lithosphere types in the Sierra Nevada, California, *in* Anderson, J.L., ed., The nature and origin of Cordilleran magmatism: Geological Society of America Memoir 174, p. 271–281.

Kistler, R.W., and Ross, D.C., 1990, A strontium isotopic study of plutons and associated rocks of the southern Sierra Nevada and vicinity, California: U.S. Geological Survey Bulletin 1920, 20 p.

Ludwig, K., 2009, Squid 2, rev. 2.50, a user's manual: Berkeley Geochronology Center Special Publication 5, 110 p.

Ludwig, K., 2012, User's manual for Isoplot 3.75, a geochronological toolkit for Microsoft Excel: Berkeley Geochronology Center Special Publication 5, 75 p.

Marcellos, A.E., and Garver, J.I., 2010, Radiation damage and uranium concentration in zircon as assessed by Raman spectroscopy and neutron irradiation: American Mineralogist, v. 95, p. 1192–1201.

McCulloh, T.H., 1952, Geology of the southern half of the Lane Mountain quadrangle, California: Los Angeles, Calif., University of California, Ph.D. dissertation, 182 p.

McCulloh, T.H., 1960, Geologic map of the Lane Mountain quadrangle, California: U.S. Geological Survey Open-File Report, 60-95, scale 1:48,000.

McDonald, E.K., 2016, Stratigraphy and detrital zircon U-Pb geochronology of the El Paso Mountains Permian metasedimentary sequence, southern California: Northridge, California State University, M.S. thesis, 124 p.

McDonald, E.K., Cecil, M.R., Marsaglia, K.M., Heermance, R.V., and Riggs, N.R., 2016a, Stratigraphy and detrital zircon geochronology of Permian deposits within the El Paso Mountains, southern California; a unique record of subduction initiation along southwestern Laurentia [abs.]: Geological Society of America Abstracts with Programs, v. 48, no. 4, https://gsa.confex.com/gsa/2016CD/webprogram/Paper274558.html.

McDonald, E.K., Cecil, M.R., Marsaglia, K.M., Heermance, R.V., and Riggs, N.R., 2016b, Stratigraphy and detrital zircon geochronology of the El Paso Mountains Permian metasedimentary sequence, southern California; a unique record of arc emergence along southwestern Laurentia [abs.]: Geological Society of America Abstracts with Programs, v. 48, no. 7, http://gsa.confex.com/gsa/2016AM/meetingapp.cgi/Paper/282233.

McDonald, E.K., Cecil, M.R., Marsaglia, K.M., and Riggs, N.R., 2018, Permian strata in the El Paso Mountains, southern California, record paleodrainage reorganization in southwestern Laurentia and the emergence of the early Cordilleran arc [abs.]: Geological Society of America Abstracts with Programs, v. 50, no. 5, https://gsa.confex.com/gsa/2018RM/meetingapp.cgi/Paper/314394.

Middlemost, E.A.K, 1994, Naming materials in the magma/igneous rock system: Earth-Science Reviews, v. 37, p. 215–224.

Miller, E.L., and Sutter, J.F., 1982, Structural geology and ^{40}Ar-^{39}Ar geochronology of the Goldstone-Lane Mountain area, Mojave Desert, California: Geological Society of America Bulletin, v. 93, p. 1191–1207.

Miller, J.S., and Glazner, A.F., 1995, Jurassic plutonism and crustal evolution in the central Mojave Desert, California: Contributions to Mineralogy and Petrology, v. 118, p. 379–395.

Miller, J.S., Glazner, A.F., Walker, J.D., and Martin, M.W., 1995, Geochronologic and isotopic evidence for Triassic-Jurassic emplacement of the eugeoclinal allochthon in the Mojave Desert region, California: Geological Society of America Bulletin, v. 107, p. 1441–1457.

Reimink, J.R., Davies, J.H.F.L., Waldron, J.W.F., and Rojas, X., 2016, Dealing with discordance; a novel approach for analysing U-Pb detrital zircon datasets: Journal of the Geological Society, v. 173, p. 577–585, https://doi.org/10.1144/jgs2015-114.

Rich, M., 1971, Fusulinids from central Mojave Desert and adjoining area, California: Journal of Paleontology, v. 45, no. 6, p. 1022–1027.

Rubatto, D., 2017, Zircon, the metamorphic mineral: Reviews in Mineralogy & Geochemistry, v. 83, p. 261–295, https://doi.org/10.2138/rmg.2017.83.9.

Saleeby, J., and Dunne, G., 2015, Temporal and tectonic relations of early Mesozoic arc magmatism, southern Sierra Nevada, California, *in* Anderson, T.H., Didenko, A.N., Johnson, C.L., Khanchuck, A.I., and MacDonald, J.H., Jr., eds., Late Jurassic margin of Laurasia—a record of faulting accommodating plate rotation: Geological Society of America Special Paper 513, p. 223–268, https://doi.org/10.1130/2015.2513(05).

Silberling, N.J., Jones, D.L., Blake, M.C., Jr., and Howell, D.G., 1987, Lithotectonic terranes of the western conterminous United States: U.S. Geological Survey Miscellaneous Field Studies Map MF-1874-C, scale 1:2,500,000, 20 p.

Silberling, N.J., Jones, D.L., Monger, J.W.H., and Coney, P.J., 1992, Lithotectonic terrane map of the North American Cordillera: U.S. Geological Survey Miscellaneous Investigations Series Map I-2176, scale 1:5,000,000.

Singleton, J.S., and Gans, P.B., 2008, Structural and stratigraphic evolution of the Calico Mountains; implications for early Miocene extension and Neogene transpression in the central Mojave Desert, California: Geosphere, v. 4, no. 3, p. 459–479, https://doi.org/10.1130/GES00143.1.

Stone, P., 2006, Preliminary geologic map of the Black Mountain area northeast of Victorville, San Bernardino County, California: U.S. Geological Survey Open-File Report 2006–1347, scale 1:12,000.

Stone, P., Barth, A.P., Wooden, J.L., Fohey-Breting, N.K., Vazquez, J.A., and Priest, S.S., 2013, Geochronologic and geochemical data from Mesozoic rocks in the Black Mountain area northeast of Victorville, San Bernardino County, California: U.S. Geological Survey Open-File Report 2013–1146, 31 p., http://pubs.usgs.gov/of/2013/1146/.

Stone, P., Brown, H.J., Cecil, M.R., Fleck, R.L., Vazquez, J.A., and Fitzpatrick, J.A., 2021, Geochronologic, isotopic, and geochemical data from pre-Cretaceous plutonic rocks in the Lane Mountain area, San Bernardino County, California: U.S. Geological Survey Open-File Report 2021–1094, 74 p, https://doi.org/10.3133/ofr20211094.

Stone, P., Brown, H.J., Cecil, M.R., Fleck, R.L., Vazquez, J.A., Fitzpatrick, J.A., and Rosario, J.J., 2019, Geochronologic, isotopic, and geochemical data from igneous rocks in the Lane Mountain area, San Bernardino County, California: U.S. Geological Survey Open-File Report 2019–1070, 34 p, https://doi.org/10.3133/ofr20191070.

Stone, P., Cecil, M.R., and Vazquez, J.A., 2023, Tabular geochronologic and geochemical data from metasedimentary and associated rocks in the Lane Mountain area, San Bernardino County, California: U.S. Geological Survey data release, https://doi.org/10.5066/P9G6YNEF.

Walker, J.D., 1987, Permian to Middle Triassic rocks of the Mojave Desert, *in* Dickinson, W.R., and Klute, M.A., eds., Mesozoic rocks of southern Arizona and adjacent areas: Arizona Geological Society Digest, v. 18, p. 1–14.

Walker, J.D., 1988, Permian and Triassic rocks of the Mojave Desert and their implications for timing and mechanism of continental truncation: Tectonics, v. 7, no. 2, p. 685–709.

Workman, B.D., 2012, Sequence stratigraphy and detrital zircon provenance of the Eureka Quartzite in south-central Nevada and eastern California: College Station, Tex., Texas A&M University, M.S. thesis, 96 p.

Appendixes

Appendix 1—Excerpts from an Unpublished Manuscript by T.H. McCulloh

The open-file geologic map of McCulloh (1960) assigns ages to the informal Carbide, Williams Well, and Noble Well formations but does not provide the basis for these age assignments. A draft manuscript by T.H. McCulloh (U.S. Geological Survey, written commun., 1960) includes detailed information on the poorly preserved fossils used to interpret the ages of these formations. A copy of this manuscript was obtained by the senior author, Paul Stone, before the present study began. Here, relevant passages of this manuscript are quoted to make this information publicly available. Such information is important for evaluating contrasts and comparisons with the detrital zircon age data provided in this report.

Excerpts of McCulloh's text are provided below, and any quoted material therein is enclosed within double quotation marks. Unpublished paleontological reports quoted by McCulloh and a quoted excerpt from Bowen (1954) are denoted by single quotation marks. Note that the manuscript does not indicate the 1954 date of publication of the Bowen report, so it is here enclosed in brackets. Geographic and locality information in the quoted text refers to the Lane Mountain 15-minute quadrangle and the Barstow 30-minute quadrangle, both of which are obsolete. The date of the manuscript is unknown, but presumably it was written around 1960, when the geologic map was published.

Carbide Formation

"All conclusions regarding the age and correlation of the Carbide formation are based fundamentally upon one small lot of poorly preserved fossils collected from recrystallized chert layers and lenses in the coarse-grained marble unit that crops out as a prominent hogback ridge in the SE ¼ of section 8, T. 11 N., R. 1 E. just west of the Barstow-Camp Irwin highway, 1.5 miles north of Jackhammer Gap in the western Calico Mountains. The following statement concerning these fossils was made by Edwin Kirk and Helen Duncan of the U.S. Geological Survey (written report dated May 26, 1953): 'This lot contains molds of crinoid stems and columnals (examined by Kirk) and indications of bryozoans (examined by Duncan). The Bryozoa are crudely silicified, but the zoarial forms suggest *Fenestella* and *Polypora,* which are common in Paleozoic and not known in Mesozoic and later rocks. According to Kirk, the crinoid stems are definitely Paleozoic types. It is our general impression that the rocks at this locality are of late Paleozoic (Carboniferous or Permian) age.'

Whereas only a suggestion can be made that the fossiliferous horizon may be Carboniferous or Permian, the conclusion is soundly established that the fossils are no older than Ordovician nor younger than Permian."

Williams Well Formation

"Crinoid stems and columnals, some of them very large, occur in coarse-grained gray marble at the eastern edge of the NE ½ of section 18, T. 12 N., R. 1 E. and 1,500 feet south of BM 2964, Lane Mountain quadrangle. According to Edwin Kirk (written communication, July 27, 1953), 'This crinoidal material is Paleozoic, not Mesozoic, and the rocks of this locality are probably of late Paleozoic age.' It can be added, that the abundance of the crinoidal material precludes a Cambrian age for the formation."

Noble Well Formation

"Despite the fact that the rocks of the Noble Well formation are thoroughly and intensely recrystallized and that they are extensively and intimately intruded by plutonic igneous rocks, fossil remains, including one fairly diagnostic mollusk, have been recovered from metamorphosed impure feldspathic sandstone interbedded with meta-conglomerate… The exact location of the fossil locality is 2,000 feet east and 800 feet south of the northwest corner of section 30, T. 12 N., R. 1 E., on the crest of the ridge extending east from hill 3731.

Most of the fossils collected are fragmentary and not identifiable. Sections of recrystallized silicified shells are abundant in a few specimens, but apparently cannot be identified. Fortunately, however, a well-preserved external mold of parts of both valves of a small pelecypod is apparently distinctive enough to permit significant conclusions regarding its affinities and age.

Paleontologists who have examined the one well-preserved specimen are agreed that it is or could be Mesozoic. P.E. Cloud (report dated July 27, 1953) supplied the following comments shortly after the specimen was submitted for identification to the U.S. Geological Survey Branch of Paleontology and Stratigraphy: 'The cast of a ribbed shell is a pelecypod of the family Cardiidae, which ranges from Triassic to Recent [Holocene] and is separated into five subfamilies. The fossil is not a protocardiinid, however, and the other four subfamilies are all post-Jurassic. The rocks at this locality are of Cretaceous or Tertiary age. This conclusion was reached in consultation with W.P. Woodridge.'

At a later date, J.B. Reeside, Jr. (report dated February 1, 1955) reported: 'Only one specimen, a mold of the exterior, shows any features of the shell. I saw this specimen when it was first submitted, but at the time it did not seem placeable, and the assignment to Cretaceous or Tertiary seemed as rational as any. Recently I have had occasion to examine the types of the genus *Septocardia* Hall and Whitfield (Paleontology, Geol. Expl. 40th Par., Rept., vol. 4, pl. 2, pp. 294–297, 1877), described from Shoshone Springs, Augusta Mountains, Nevada, and assigned to the Jurassic but now known to be Triassic. Though the hinge of the California specimen is not available, and identification is therefore somewhat dubious, the similarities to *Septocardia* are great enough that I think the specimen can be called *Septocardia*? and the age placed as probably Triassic.'

Professor S.W. Muller of Stanford University (written communication, November 10, 1953) writes: 'The latex casts of

the specimens look like some form of a Cardiid. There is some similarity to the *Cardita*-like form from the Karnian [Triassic] of northern Nevada, but positive identification cannot be made because the hinge is not available. The *Cardita*-like form has been described in the 40th parallel survey report on the generic name, *Septocardium*, and recently Cox of the British Museum reported from the Triassic of Peru, the genus *Pascoella*."

Because of his uncertainty, Muller referred the specimen to Dr. Myra Keen who supplied the following comment (statement quoted in a letter dated November 10, 1953 and signed by S.W. Muller): 'The specimen has a hinge that could be interpreted as Cardiid. There are several stocks of this pelecypod family (Cardiidae) that range back to the Jurassic, one even to U. [Upper] Triassic. The sculpture of the specimen is suggestive of an unnamed stock of the Subfamily Cardiinae from the Cretaceous. *Cardium paupereculum* Meek [1871] is a good representative of this group, the range of which is lower to upper Cretaceous.'

The oldest age suggested by the paleontologists quoted above for the fossils from the Noble Well formation is Triassic, with no indication that they might be Paleozoic. The youngest possible age range suggested is Cretaceous and Tertiary. The fact that uppermost Cretaceous and Paleocene sedimentary rocks rest noncomformably in many other places in California upon plutonic igneous rocks comparable in all respects to those that intrude the Noble Well formation we consider to be satisfactory evidence that the Noble Well formation can be considered no younger than older Upper [Late] Cretaceous.

In view of the lack of confidence expressed by each of the paleontologists quoted above in their attempts to assign an exact age to the single well-preserved mold, and in view of the lack of complete agreement among the several scientists as to the most probable age range of the form, it appears to this writer that the fairest summary of current opinion is that the fossil and the rocks from which it was collected are Mesozoic in age, and that they are most likely Triassic in age, but that a Jurassic or even a Cretaceous age has not been ruled out entirely."

Suggested Correlation of the Noble Well Formation with the Fairview Valley Formation of Bowen (1954)

"The only formation in the central Mojave Desert that is known by the author to contain rocks closely resembling those of the Noble Well formation is the Fairview Valley formation of Bowen [1954]. The Fairview Valley formation, which is known only in the eastern part of the Barstow quadrangle 30 miles south of Lane Mountain, consists of 6,075 feet of metamorphosed limestone, limy siltstone, arkosic and feldspathic sandstone, and conglomerate, much of it limestone conglomerate. Limestone clasts in almost unrecrystallized parts of the limestone conglomerate yielded abundant late Paleozoic fossils and permitted Bowen [1954] to write, 'The Fairview Valley formation is certainly younger than Pennsylvanian and most probably younger than Lower [early] Permian. It is older than the intruding Jura-Cretaceous [Jurassic to Cretaceous] granitic rocks and older than the Triassic(?) Sidewinder Volcanic series. In the absence of Mesozoic fossils, it must be presumed to be Upper [late] Permian.'

The metamorphosed limestone conglomerate of the Fairview Valley formation is like the recrystallized limestone conglomerate of the Noble Well formation in every respect except degree of metamorphism and its content of fossils. The feldspathic and arkosic meta-sandstones of the lower part of the Fairview Valley formation are also matched by the metamorphosed arkosic sands of the Noble Well formation. Finally, the possible age ranges of the two formations are not very different. The Noble Well formation is surely Mesozoic, whereas the Fairview Valley formation is Mesozoic or late Permian. Because of their lithologic similarities and the possibility of their age equivalence, the writer suggests that the possibility be entertained that the two formations are correlative.

The reader can judge from what has been written in the preceding paragraphs that the occurrence of Mesozoic fossils in rocks of the Noble Well formation is unique in an area of tens of thousands of square miles. The possible paleogeographic consequences of its occurrence could therefore be exceedingly important. The need for more precise dating of the Noble Well formation is obvious."

References Cited

Bowen, O.E., Jr., 1954, Geology and mineral deposits of Barstow quadrangle, San Bernardino County, California: California Division of Mines Bulletin 165, p. 5–185, scale 1:125,000.

McCulloh, T.H., 1960, Geologic map of the Lane Mountain quadrangle, California: U.S. Geological Survey Open-File Report, 60-95, scale 1:48,000

Appendix 2—Methods of U-Pb Zircon Geochronology

LA-SF-ICPMS Analyses (California State University, Northridge)

Zircon separates received from the U.S. Geological Survey were poured or picked onto double sided tape, mounted in epoxy, ground, and polished. They were then imaged on a Gatan MiniCL detector attached to a FEI Quanta 600 scanning electron microscope.

For most analyses, uranium-lead ratios were collected using a ThermoScientific Element2 sector field inductively coupled plasma mass spectrometer (SF-ICPMS) coupled with a New Wave/Lambda Physik DUV193 Excimer laser (operating at a wavelength of 193 nanometers). Prior to analysis the Element2 was tuned using the NIST 612 glass standard to optimize signal intensity and stability. Laser beam diameter was ~30–40 microns at 10 Hz and 75–100 percent power. Ablation was performed in a New Wave SuperCell and sample aerosol was transported with helium carrier gas through Teflon-lined tubing, where it was mixed with Ar gas before introduction to the plasma torch. Flow rates for Ar and He gases were as follows: Ar cooling gas (16.0 nanoliter/min), Ar auxiliary gas (1.0 nanoliter/min), He carrier gas (~0.3-0.5 nanoliter/min), Ar sample gas (1.1-1.3 nanoliter/min). Isotope data were collected in E-scan mode with magnet set at mass 202, and RF Power at 1245 W. Isotopes measured include ^{202}Hg, ^{204}(Pb+Hg), ^{206}Pb, ^{207}Pb, ^{208}Pb, ^{232}Th, and ^{238}U. All isotopes were collected in counting mode with the exception of ^{232}Th and ^{238}U which were collected in analogue mode. Analyses were conducted in a ~40-minute time resolved analysis mode. Each zircon analysis consisted of a 10-second integration on peaks with the laser on but not ablating (for backgrounds), 20 seconds of integrations with the laser firing on sample, and a 5–10 second delay to purge the previous sample and move to the next sample. Approximate depth of the ablation pit was ~20–30 microns.

For analyses conducted toward the end of the study, the Element2 was coupled with a Teledyne Cetec Analyte G2 Excimer laser with a laser beam diameter of ~25 microns, and ablation was performed in a HelEx II Active 2-Volume Cell. Each zircon analysis consisted of a 20-second integration with the laser firing on sample, and a 20-second delay to purge the previous sample and move to the next sample.

The primary standard, 91500, was analyzed every 5–15 analyses to correct for in-run fractionation of Pb/U and Pb isotopes. One or two secondary zircon standards (Temora-2, Plesovice, and [or] R33) were analyzed every ~10 analyses to assess reproducibility of the data.

Analytical data reduction utilized iolite software. Corrections for minor amounts of common Pb in zircons <1,400 Ma were made using the "Age7corr" function in Isoplot 3.75 (Ludwig, 2012) with an assumed initial ^{207}Pb/^{206}Pb ratio of 0.86 (Stacey and Kramers, 1975). This calculation yielded the "207-corrected age," which was reported as the final age for zircons <1,400 mega-annum (Ma). The uncorrected ^{207}Pb/^{206}Pb age was used as the final age for zircons >1,400 Ma.

Percent discordance was calculated for all age results. For zircons >1,400 Ma, discordance was calculated as the percent difference between the ^{207}Pb/^{206}Pb age and the ^{206}Pb/^{238}U age. For zircons <1,400 Ma, discordance was calculated as the percent difference between the ^{207}Pb/^{235}U age and the ^{206}Pb/^{238}U age. Some of the most highly discordant grains were apatites that were inadvertently analyzed along with zircons in some very fine-grained samples.

SHRIMP-RG Analyses (Stanford)

Individual zircons were mounted in epoxy, polished, and coated with gold prior to analysis. Cathodoluminescence images were used to select relatively homogeneous spots within compositionally zoned zircons. Analytical conditions for the sensitive high resolution ion microprobe analyses were ~4–6 nanoampere primary beam of negatively charged O_2 ions. Secondary ions were measured by peak hopping using a single electron multiplier collector. The mass spectrometer was tuned to a mass resolution of ~6000, sufficient to resolve any significant interferences. Intensities of secondary ion peaks of Zr_2O^+, ^{204}Pb$^+$, background, ^{206,207,208}Pb$^+$, ^{238}U$^+$, ^{232}Th$^+$, and ^{238}U^{16}O$^+$ were collected in five scans and corrected for collector deadtime. U/Pb ratios were calibrated to Temora-2 zircon using an age of 418.4 Ma (Mattinson, 2010) employing the U/Pb–UO/U calibration typical for ion microprobe U-Pb geochronology (Williams, 1998). Uranium and thorium concentrations were calibrated to MAD-559 zircon (Coble and others, 2018).

Analytical data reduction utilized the software programs Squid 2 version 2.51 and Isoplot version 3.76 (Ludwig, 2009, 2012). The data reduction routine yielded several different isotopic ages, all of which included a common lead correction using the values of Stacey and Kramers (1975). Preferred ages are reported as the 204-corrected ^{207}Pb/^{206}Pb age for grains >1,400 Ma and the 207-corrected ^{206}Pb/^{238}U age for grains <1,400 Ma.

For consistency with the ICP-AES-MS analyses, percent discordance was calculated for all age results. For zircons >1,400 Ma, discordance was calculated as the percent difference between the 204-corrected ^{207}Pb/^{206}Pb age and the 204-corrected ^{206}Pb/^{238}U age. For zircons <1,400 Ma, discordance was calculated as the percent difference between the 204-corrected ^{207}Pb/^{235}U age and the 204-corrected ^{206}Pb/^{238}U age. Note that the ^{207}Pb/^{235}U ages were calculated using IsoplotR (Vermeesch, 2018).

References Cited

Coble, M. A., Vazquez, J.A., Barth, A.P., Wooden, J.L., Burns, D., Kylander-Clark, A., Jackson, S., and Vennari, C.E., 2018, Trace element characterisation of MAD-559 zircon reference material for ion microprobe analysis: Geostandards and Geoanalytical Research, v. 42, no. 4, p. 481–497, https://doi.org/10.1111/ggr.12238.

Ludwig, K., 2009, Squid 2, rev. 2.50, a user's manual: Berkeley Geochronology Center Special Publication 5, 110 p.

Ludwig, K., 2012, User's manual for Isoplot 3.75, a geochronological toolkit for Microsoft Excel: Berkeley Geochronology Center Special Publication 5, 75 p.

Mattinson, J.M, 2010, Analysis of the relative decay constants of ^{235}U and ^{238}U by multi-step CA-TIMS measurements of closed-system natural zircon samples: Chemical Geology, v. 275, p. 186–198.

Stacey, J.S., and Kramers, J.D., 1975, Approximation of terrestrial lead isotope evolution by a two-stage model: Earth and Planetary Science Letters, v. 26, p. 207–221.

Vermeesch, P., 2018, IsoplotR, a free and open toolbox for geochronology: Geoscience Frontiers, v. 9, p. 1479–1493, https://doi.org/10.1016/j.gsf.2018.04.001.

Williams, I.S., 1998, U-Th-Pb geochronology by ion microprobe: Reviews in Economic Geology, v. 7, p. 1–35.

Moffett Field Publishing Science Center
Manuscript approved December 9, 2022
Edited by Mitchell Phillips
Layout by Cory Hurd

ISSN 2331-1258 (online)
https://doi.org/10.3133/ofr20221115